Journal of Computational and Applied Mathematics 465 (2025) 116582

Contents lists available at ScienceDirect

Journal of Computational and Applied Mathematics

journal homepage: www.elsevier.com/locate/cam

A locking-free conforming discontinuous Galerkin finite element method for linear elasticity problems

Fuchang Huo [a,*], Weilong Mo [a], Yulin Zhang [b]

[a] School of Mathematics, Jilin University, Changchun 130012, PR China
[b] School of Mathematical Sciences and Institute of Natural Sciences, Shanghai Jiao Tong University, Shanghai 200240, PR China

ARTICLE INFO

MSC:
65N30
65N15
74S05
74B05
35J50

Keywords:
Conforming discontinuous Galerkin finite element methods
Weak gradient
Weak divergence
Linear elasticity
Locking-free

ABSTRACT

This paper proposes a locking-free conforming discontinuous Galerkin (CDG) numerical scheme for solving linear elasticity problems. By introducing the discrete weak strain and discrete weak stress tensors, this paper establishes two types of numerical methods based on the primal and mixed variational formulations. The weak differential operators are approximated using discontinuous polynomials on each local element. Locking-free error estimates of optimal order convergence are established in both the energy norm and the L^2-norm, demonstrating the locking-free property of the CDG schemes, which arises from their equivalence. Numerical results are presented to confirm the accuracy and locking-free property of the CDG schemes.

1. Introduction

The linear elasticity problem is a fundamental model extensively employed in solid mechanics. This model finds wide-ranging applications in engineering and various scientific fields, such as engineering mechanics [1], porous media flow [2], and so on. Finding effective and robust numerical methods to solve linear elasticity problems is a topic of great interest.

In the past few years, various numerical methods have been proposed for linear elasticity problems, such as finite difference and boundary integral methods (FDM & BIM) [3,4], finite element methods (FEM) [5–7], mixed finite element methods (MFEM) [8–11], discontinuous Galerkin (DG) methods [12–14], virtual element methods (VEM) [15–17], weak Galerkin (WG) methods [18–21], etc. Their developments lead to advancements in computational methods and facilitate the analysis and design of complex systems and structures.

This paper focuses on developing efficient new numerical methods for solving linear elasticity equations by utilizing the conforming discontinuous Galerkin (CDG) method, which has been recently proposed and developed in [22–26]. Consider an open, bounded, and connected domain Ω in $\mathbb{R}^d$ $(d = 2, 3)$. This domain possesses a Lipschitz continuous boundary denoted as $\partial\Omega$. We examine an elastic body subjected to an external force $\boldsymbol{f}$ and a homogeneous displacement boundary condition. In this context, the governing equation for its kinematic behavior is as follows:

* Corresponding author.
E-mail addresses: huofc22@mails.jlu.edu.cn (F. Huo), mowl22@mails.jlu.edu.cn (W. Mo), yulin.zhang@sjtu.edu.cn (Y. Zhang).

https://doi.org/10.1016/j.cam.2025.116582
Received 18 December 2023; Received in revised form 30 December 2024
Available online 20 February 2025

Definition 1.1 (*Linear Elasticity Problem*)**.** Find a displacement field $\boldsymbol{u}$ that satisfies

$$-\nabla \cdot \sigma(\boldsymbol{u}) = \boldsymbol{f}, \quad \text{in } \Omega, \tag{1.1a}$$

$$\boldsymbol{u} = \boldsymbol{0}, \quad \text{on } \partial\Omega, \tag{1.1b}$$

where $\boldsymbol{f}$ denotes the external force, $\sigma(\boldsymbol{u})$ represents the Cauchy stress tensor

$$\sigma(\boldsymbol{u}) := 2\mu\varepsilon(\boldsymbol{u}) + \lambda(\nabla \cdot \boldsymbol{u})\mathbb{I}, \tag{1.2}$$

here $\varepsilon(\boldsymbol{u}) := \frac{1}{2}(\nabla\boldsymbol{u} + \nabla\boldsymbol{u}^T)$ is the linear strain tensor, $\mathbb{I}$ is $d \times d$ identity matrix, μ, λ are the Lamé constants defined by

$$\mu = \frac{E}{2(1+\nu)}, \quad \lambda = \frac{E\nu}{(1+\nu)(1-2\nu)}, \tag{1.3}$$

where $E \in (0, \infty)$ is the Young's modulus, $\nu \in (0, \frac{1}{2})$ is the Poisson ratio.

Denote by $(\cdot, \cdot)$ the L^2-inner product in $L^2(\Omega), [L^2(\Omega)]^d, [L^2(\Omega)]^{d\times d}$ and by $H^s(\Omega)\,(s \geq 0)$ the standard Sobolev space:

$$H^s(\Omega) := \{v : v \in L^2(\Omega),\ \partial^\alpha v \in L^2(\Omega), |\alpha| \leq s\}. \tag{1.4}$$

$H_0^s(\Omega)$ be the closed subspace of $H^s(\Omega)$ defined by $H_0^s(\Omega) := \{v : v \in H^s(\Omega),\ v|_{\partial\Omega} = 0\}$, $\|\cdot\|_s, |\cdot|_s$ be the associated norms and semi-norms in $H^s(\Omega)$. The corresponding variational formulation of (1.1) reads as follows:

Proposition 1.1 (*Variational Formulation*)**.** *Find* $\boldsymbol{u} \in [H_0^1(\Omega)]^d$ *satisfying*

$$(2\mu\varepsilon(\boldsymbol{u}), \varepsilon(\boldsymbol{v})) + (\lambda\nabla \cdot \boldsymbol{u}, \nabla \cdot \boldsymbol{v}) = (\boldsymbol{f}, \boldsymbol{v}), \tag{1.5}$$

for all $\boldsymbol{v} \in [H_0^1(\Omega)]^d$.

This paper's principal objective is to present a novel conforming discontinuous Galerkin (CDG) method tailored for solving linear elasticity problems (1.1). The CDG method based on the weak Galerkin (WG) method [27] was first proposed by Ye and Zhang in 2020 [24]. It preserves the core idea of the WG method, which uses the discrete weak differential operators to approximate classical differential operators in the variational formulation, and it eliminates the requirement of the stabilizers in the WG method [24–26] by increasing the degree of the polynomials used for approximating discrete weak differential operators.

Locking usually occurs when the mathematical formulation of a certain problem requires a high parameter dependency. For linear elasticity problems, locking occurs when $\lambda \to \infty$ (or equivalently, $\nu \to \frac{1}{2}$), indicating that the elastic body becomes nearly incompressible and causing numerical schemes turn to be unstable [28,29]. Various numerical discretization methods have been presented to address locking, including nonconforming finite element methods [6,30,31], mixed finite element methods [32–34], discontinuous Galerkin methods [13,35,36], virtual element methods [15,16,37], and weak Galerkin methods [18,19,21,38–40]. [6] devised a locking-free nonconforming adaptive finite element algorithm by using Crouzeix–Raviart element. [30] constructed locking-free second-order elements on triangular and rectangular grids. [31] presented a locking-free nonconforming element employing a mixed formulation on simplicial grids. These nonconforming elements are constructed based on simple grids. [32–34] proposed mixed finite elements based on the Hellinger–Reissner principle on simplicial grids, which are locking-free. However, these mixed finite element methods require more unknowns and result in saddle-point problems. [13] constructed locking-free interior penalty discontinuous Galerkin methods for incompressible and nearly incompressible elasticity problems on triangular grids using Nitsche's method. These methods introduce too many unknowns. [35,36] presented hybridizable discontinuous Galerkin finite element methods for linear elasticity problems with strong symmetric stress tensor. [15,16,37] developed locking-free virtual element methods for linear elasticity problems on polygonal or polyhedral grids. [19,38] devised locking-free weak Galerkin methods by introducing pseudo-pressure on polygonal or polyhedral grids. [18,39,40] proposed lowest-order weak Galerkin methods for the linear elasticity based on the grad-div formulation. [21] presented a locking-free weak Galerkin solver without a penalty term on quadrilateral grids. Overall, the above methods overcome locking. This article focuses on developing a locking-free, simple, and flexible numerical method on arbitrary polygonal or polyhedral grids.

In this paper, we present the conversion of the primal formulation (1.5) into a mixed formulation (4.1) by introducing the hydrostatic pressure variable. We have developed two CDG schemes, one originating from the primal formulation (1.5) and the other from the mixed formulation (4.1). The CDG method is applied to the linear elasticity problems based on the mixed formulation (4.1), which results in a locking-free numerical approximation for the displacement field. Surprisingly, we have identified an equivalence between CDG schemes derived from both the primal formulation (1.5) and the mixed formulation (4.2). This observation raises the possibility that based on the primal formulation, the CDG scheme (3.3) could be immune to locking phenomena.

The structure of the rest of this paper is as follows. In Section 2, we introduce the definitions and properties of the discrete weak gradient and weak divergence for vector-valued functions. In Section 3, we construct a CDG approach designed for the treatment of linear elasticity problems based on the primal formulation (1.5). In Section 4, we propose another form of the CDG scheme based on the mixed formulation (4.2) and prove the equivalence between the two CDG methods. In Section 5, we prepare for the subsequent error analysis by deriving the error equations and some related inequalities. In Section 6, an error estimate of optimal order within a discrete H^1-norm is derived. In Section 7, we employ the standard duality argument method to establish the optimal error estimate for the displacement variable in the L^2-norm. Section 8 presents some numerical results to substantiate the effectiveness and locking-free property of the proposed methods for the linear elasticity problems. Section 9 summarizes the paper and provides some conclusions. Finally, in Appendix, some useful tools and estimates for the error analysis are given.

2. Weak divergence and weak gradient operators

In this section, we present the definitions of two types of weak discrete differential operators.

Let $\mathcal{T}_h$ be a shape regular partition [41,42] of the domain $\Omega \subset \mathbb{R}^d$ $(d = 2,3)$ that consists of polygon (2D) or polyhedra (3D). Denote by $\mathcal{E}_h$ the set of all edges (2D) or faces (3D) in $\mathcal{T}_h$ and $\mathcal{E}_h^0$ the set of all interior edges (2D) or faces (3D). For $T \in \mathcal{T}_h$, let h_T be the diameter of T. Denote by $h = \max_{T\in\mathcal{T}_h} h_T$ the mesh size h of $\mathcal{T}_h$.

The weak finite element space denoted as V_h is formally defined as:

$$V_h := \{\boldsymbol{v} \in [L^2(\Omega)]^d : \boldsymbol{v}|_T \in [P_k(T)]^d,\ \forall T \in \mathcal{T}_h,\ k \geq 1\}. \tag{2.1}$$

Let T_1, T_2 be two polygon/polyhedra sharing edge (2D) or face (3D) $e \in \mathcal{E}_h^0$. For a vector-valued function $\boldsymbol{v} \in V_h + [H_0^1(\Omega)]^d$, the average $\{\cdot\}$ and jump $[\cdot]$ are defined as follows:

$$\begin{aligned}
\{\boldsymbol{v}\} &= \begin{cases} \frac{1}{2}(\boldsymbol{v}|_{T_1} + \boldsymbol{v}|_{T_2}), & e \in \mathcal{E}_h^0, \\ \mathbf{0}, & e \subset \partial\Omega, \end{cases} \\
[\boldsymbol{v}] &= \begin{cases} \boldsymbol{v}|_{T_1} - \boldsymbol{v}|_{T_2}, & e \in \mathcal{E}_h^0, \\ \boldsymbol{v}|_e, & e \subset \partial\Omega. \end{cases}
\end{aligned} \tag{2.2}$$

According the definitions of $\{\cdot\}$ and $[\cdot]$, it is straightforward to show that

$$\begin{aligned}
\|\boldsymbol{v} - \{\boldsymbol{v}\}\|_e &= \|[\boldsymbol{v}]\|_e, \qquad e \in \partial\Omega, \\
\|\boldsymbol{v} - \{\boldsymbol{v}\}\|_e &= \frac{1}{2}\|[\boldsymbol{v}]\|_e, \quad e \in \mathcal{E}_h^0.
\end{aligned} \tag{2.3}$$

Then we give the definitions of the discrete weak gradient and weak divergence operators [42,43].

Definition 2.1 (*[42,43], Discrete Weak Gradient*)**.** For any $T \in \mathcal{T}_h$ and $\boldsymbol{v} \in V_h + [H_0^1(\Omega)]^d$, the discrete weak gradient operator $\nabla_w : V_h + [H_0^1(\Omega)]^d \to [P_j(T)]^{d\times d}$ $(j > k)$ is defined as the unique matrix-valued polynomial in $[P_j(T)]^{d\times d}$ satisfying

$$(\nabla_w \boldsymbol{v}, \varphi)_T = -(\boldsymbol{v}, \nabla\cdot\varphi)_T + \langle\{\boldsymbol{v}\}, \varphi\cdot\boldsymbol{n}\rangle_{\partial T}, \qquad \forall\, \varphi \in [P_j(T)]^{d\times d}, \tag{2.4}$$

where $\boldsymbol{n}$ is unit outward normal vector on ∂T.

Definition 2.2 (*[42,43], Discrete Weak Divergence*)**.** For any $T \in \mathcal{T}_h$ and $\boldsymbol{v} \in V_h + [H_0^1(\Omega)]^d$, its discrete weak divergence $\nabla_w \cdot \boldsymbol{v} \in P_{k-1}(T)$ satisfying

$$(\nabla_w \cdot \boldsymbol{v}, p)_T = -(\boldsymbol{v}, \nabla p)_T + \langle\{\boldsymbol{v}\}\cdot\boldsymbol{n}, p\rangle_{\partial T}, \qquad \forall\, p \in P_{k-1}(T), \tag{2.5}$$

where $\boldsymbol{n}$ is unit outward normal vector on ∂T.

Remark 2.1. The choice of j in the definition of ∇_w depends on the number of edges/faces of polygon/polyhedron. In general, $j = n + k - 1$, where n is the number of edges/faces of polygon/polyhedron. For the choice of k, we require $k \geq 1$, as outlined in (2.1).

3. Numerical algorithm

This section is devoted to establishing the CDG scheme for the primal linear elastic problems (1.1).

We give the definitions of the weak strain tensor and weak Cauchy stress tensor:

$$\varepsilon_w(\boldsymbol{u}) := \frac{1}{2}\left(\nabla_w \boldsymbol{u} + \nabla_w \boldsymbol{u}^T\right), \tag{3.1a}$$

$$\sigma_w(\boldsymbol{u}) := 2\mu\varepsilon_w(\boldsymbol{u}) + \lambda(\nabla_w\cdot\boldsymbol{u})\mathbb{I}, \tag{3.1b}$$

and introduce a bilinear form

$$\begin{aligned}
\mathcal{A}(\boldsymbol{u},\boldsymbol{v}) &= 2\mu\,(\varepsilon_w(\boldsymbol{u}), \varepsilon_w(\boldsymbol{v})) + \lambda\,(\nabla_w\cdot\boldsymbol{u}, \nabla_w\cdot\boldsymbol{v}) \\
&= 2\mu\sum_{T\in\mathcal{T}_h}(\varepsilon_w(\boldsymbol{u}), \varepsilon_w(\boldsymbol{v}))_T + \lambda\sum_{T\in\mathcal{T}_h}(\nabla_w\cdot\boldsymbol{u}, \nabla_w\cdot\boldsymbol{v})_T.
\end{aligned} \tag{3.2}$$

Now we present the CDG scheme for solving the primal linear elastic problems:

Weak Galerkin Algorithm 1. *Seek $\boldsymbol{u}_h \in V_h$ satisfying*

$$\mathcal{A}(\boldsymbol{u}_h, \boldsymbol{v}) = (\boldsymbol{f}, \boldsymbol{v}), \qquad \forall\, \boldsymbol{v} \in V_h. \tag{3.3}$$

Next, we shall delve into the well-posedness analysis of the presented CDG scheme (3.3).

Lemma 3.1 ([25]). *Let T be a convex $(n+1)$-polygon/polyhedron of size h_T with edges/faces $e, e_1, \dots, e_n$. Given a polynomial $\varphi_0 \in P_k(e)$, we define the polynomial $\varphi = \lambda_1 \cdots \lambda_n \varphi_0 \in P_{k+n}(T)$ such that it satisfies*

$$\langle \varphi - \varphi_0, \phi \rangle_e = 0, \qquad \forall \phi \in P_k(e), \tag{3.4a}$$

$$(\varphi, \phi)_T = 0, \qquad \forall \phi \in P_{k-1}(T), \tag{3.4b}$$

where $\lambda_i \in P_1(T)$ is such that it equals zero on e_i and takes the value of 1 at the barycenter of e. Then, there exists a constant $C > 0$ independent of T or φ_0 such that

$$\|\varphi\|_T \le C h_T^{1/2} \|\varphi_0\|_e. \tag{3.5}$$

Proof. For a detailed proof, refer to [25]. □

Lemma 3.2. *For any $\boldsymbol{v} \in V_h$, we have*

$$\|\boldsymbol{v} - \{\boldsymbol{v}\}\|_{\partial T}^2 \le C h_T \, \|\varepsilon_w(\boldsymbol{v})\|_T^2, \tag{3.6}$$

where $C > 0$ is independent of the mesh size h.

Proof. For any $\boldsymbol{v} \in V_h$ and $\tau \in [P_j(T)]^{d\times d}$ (for simplicity, assume $d = 2$), by the definition of discrete weak gradient and integration by parts, it follows that

$$\begin{aligned} (\nabla_w \boldsymbol{v}, \tau)_T &= -(\boldsymbol{v}, \nabla \cdot \tau)_T + \langle \{\boldsymbol{v}\}, \tau \cdot \boldsymbol{n} \rangle_{\partial T} \\ &= (\nabla \boldsymbol{v}, \tau)_T - \langle \boldsymbol{v} - \{\boldsymbol{v}\}, \tau \cdot \boldsymbol{n} \rangle_{\partial T}. \end{aligned} \tag{3.7}$$

Suppose $\boldsymbol{v} = [v^{(1)}, v^{(2)}]^T, \{\boldsymbol{v}\} = [\bar{v}^{(1)}, \bar{v}^{(2)}]^T$. Taking $\varphi_0^{(i)} = v^{(i)} - \bar{v}^{(i)}$ $(i = 1, 2)$ in Lemma 3.1, then there exist $\varphi^{(1)}, \varphi^{(2)} \in P_{k+n-1}(T)$ such that (3.4) holds. Without losing generality, suppose $\boldsymbol{n} = [n_1, n_2]^T$, $n_i \neq 0$, choose $\boldsymbol{\phi}_0^{(1)} = [\varphi^{(1)}/n_1, 0]^T, \boldsymbol{\phi}_0^{(2)} = [0, \varphi^{(2)}/n_2]^T$, then there exists a matrix-value function $\tau_0 = [\boldsymbol{\phi}_0^{(1)}, \boldsymbol{\phi}_0^{(2)}] \in [P_j(T)]^{2\times 2}, j = k + n - 1$ by (3.4)–(3.5) such that

$$(\nabla \boldsymbol{v}, \tau_0)_T = 0, \tag{3.8a}$$

$$\langle \boldsymbol{v} - \{\boldsymbol{v}\}, \tau_0 \cdot \boldsymbol{n} \rangle_{\partial T \backslash e} = 0, \tag{3.8b}$$

$$\langle \{\boldsymbol{v}\} - \boldsymbol{v}, \tau_0 \cdot \boldsymbol{n} \rangle_e = \|\boldsymbol{v} - \{\boldsymbol{v}\}\|_e^2, \tag{3.8c}$$

and

$$\|\tau_0\|_T \le C h_T^{1/2} \|\boldsymbol{v} - \{\boldsymbol{v}\}\|_e. \tag{3.9}$$

In particular, one can see that $\tau_0 = \tau_0^T$ from its definition.

Then, for any $\tau \in [P_j(T)]^{2\times 2}$, by using the definition of weak strain and integration by parts, we have

$$\begin{aligned} (\varepsilon_w(\boldsymbol{v}), \tau)_T &= \frac{1}{2}(\nabla_w \boldsymbol{v}, \tau)_T + \frac{1}{2}(\nabla_w \boldsymbol{v}^T, \tau)_T \\ &= \frac{1}{2}(\nabla_w \boldsymbol{v}, \tau + \tau^T)_T \\ &= -\frac{1}{2}(\boldsymbol{v}, \nabla \cdot (\tau + \tau^T))_T + \frac{1}{2}\langle \{\boldsymbol{v}\}, (\tau + \tau^T) \cdot \boldsymbol{n} \rangle_{\partial T} \\ &= \frac{1}{2}(\nabla \boldsymbol{v}, \tau + \tau^T)_T - \frac{1}{2}\langle \boldsymbol{v} - \{\boldsymbol{v}\}, (\tau + \tau^T) \cdot \boldsymbol{n} \rangle_{\partial T}. \end{aligned} \tag{3.10}$$

Taking $\tau = \tau_0$ in (3.10), we get

$$(\varepsilon_w(\boldsymbol{v}), \tau_0)_T = (\nabla \boldsymbol{v}, \tau_0)_T - \langle \boldsymbol{v} - \{\boldsymbol{v}\}, \tau_0 \cdot \boldsymbol{n} \rangle_{\partial T}, \tag{3.11}$$

i.e.

$$(\varepsilon_w(\boldsymbol{v}), \tau_0)_T = \|\boldsymbol{v} - \{\boldsymbol{v}\}\|_e^2. \tag{3.12}$$

By using the Cauchy–Schwarz inequality and (3.9), we arrive at

$$\|\boldsymbol{v} - \{\boldsymbol{v}\}\|_e^2 \le C\|\varepsilon_w(\boldsymbol{v})\|_T \|\tau_0\|_T \le C h_T^{1/2} \, \|\varepsilon_w(\boldsymbol{v})\|_T \|\boldsymbol{v} - \{\boldsymbol{v}\}\|_e,$$

which leads to

$$\|\boldsymbol{v} - \{\boldsymbol{v}\}\|_e \le C h_T^{1/2} \, \|\varepsilon_w(\boldsymbol{v})\|_T.$$

This completes the proof. □

Then, we give the definition of RM (rigid motion) space

$$RM(\Omega) = \{\boldsymbol{a} + \eta \boldsymbol{x} : \boldsymbol{a} \in \mathbb{R}^d, \eta \in SK(d)\}, \tag{3.13}$$

where $\boldsymbol{x}$ is the position vector, $SK(d)$ is the set of skew-symmetric $d \times d$ matrices. $RM(\Omega)$ can be viewed as the kernel space of the strain tensor, i.e., for any $\boldsymbol{v} \in [H^1(\Omega)]^d$,

$$\varepsilon(\boldsymbol{v}) = 0 \Leftrightarrow \boldsymbol{v} \in RM(\Omega). \tag{3.14}$$

Theorem 3.1 (*Well-posedness*)**.** *There exists a unique solution of the CDG scheme (3.3).*

Proof. In finite-dimensional systems, we only need to prove uniqueness. Let $\boldsymbol{u}_h^i$ $(i = 1, 2)$ be the two solution of the CDG scheme (3.3), then we have

$$\mathcal{A}(\boldsymbol{u}_h^i, \boldsymbol{v}) = (\boldsymbol{f}, \boldsymbol{v}), \qquad \forall \boldsymbol{v} \in V_h.$$

Letting $\boldsymbol{w} = \boldsymbol{u}_h^1 - \boldsymbol{u}_h^2$, we get

$$\mathcal{A}(\boldsymbol{w}, \boldsymbol{v}) = 0, \qquad \forall \boldsymbol{v} \in V_h. \tag{3.15}$$

By setting $\boldsymbol{v} = \boldsymbol{w}$ in (3.15), we arrive at

$$\mathcal{A}(\boldsymbol{w}, \boldsymbol{w}) = 0,$$

which leads to

$$\varepsilon_w(\boldsymbol{w}) = \boldsymbol{0}, \quad \text{in } T, \tag{3.16}$$

$$\nabla_w \cdot \boldsymbol{w} = 0, \quad \text{in } T. \tag{3.17}$$

From (3.16) and Lemma 3.2, we have $\boldsymbol{w} = \{\boldsymbol{w}\}$ on ∂T, which implies that $\boldsymbol{w}$ is continuous on the entire Ω.

Using the definition of weak strain and integration by parts, we get

$$(\varepsilon_w(\boldsymbol{w}), \tau)_T = \frac{1}{2}(\nabla \boldsymbol{w}, \tau + \tau^T)_T = (\varepsilon(\boldsymbol{w}), \tau)_T, \qquad \forall \tau \in [P_j(T)]^{d \times d}, T \in \mathcal{T}_h, \tag{3.18}$$

thus $\varepsilon(\boldsymbol{w}) = 0$, which implies that $\boldsymbol{w} \in RM(T)$ for all $T \in \mathcal{T}_h$. For any adjacent elements T_1, T_2, according to $\boldsymbol{w}|_{T_i} \in RM(T_i)$, we have

$$\boldsymbol{w}|_{T_i} = \boldsymbol{a}_i + \eta_i \boldsymbol{x}, \qquad \eta_i \in SK(d).$$

From the fact that $\boldsymbol{w}$ is continuous on the entire Ω, we get

$$\boldsymbol{a}_1 + \eta_1 \boldsymbol{x} = \boldsymbol{a}_2 + \eta_2 \boldsymbol{x} \text{ on } T_1 \cap T_2 \Rightarrow \boldsymbol{a}_1 = \boldsymbol{a}_2, \eta_1 = \eta_2,$$

which implies that $\boldsymbol{w} \in RM(T_1 \cup T_2)$, thus $\boldsymbol{w} \in RM(\Omega)$. Since $\boldsymbol{w}|_{\partial\Omega} = \boldsymbol{0}$, together with the Korn's inequality [19,29], we have $\boldsymbol{w} = \boldsymbol{0}$ in Ω. The proof of the theorem is completed. □

4. An equivalent mixed formulation

To overcome the locking phenomena in the primal problem (1.1) as $\lambda \to \infty$, we reformulate (1.1) into the following generalized Stokes equations:

$$-\nabla \cdot (2\mu\varepsilon(\boldsymbol{u})) - \nabla p = \boldsymbol{f}, \qquad \text{in } \Omega, \tag{4.1a}$$

$$\nabla \cdot \boldsymbol{u} = \lambda^{-1} p, \quad \text{in } \Omega, \tag{4.1b}$$

$$\boldsymbol{u} = \boldsymbol{0}, \qquad \text{on } \partial\Omega, \tag{4.1c}$$

with the compatibility condition $\int_\Omega p \, \mathrm{d}\boldsymbol{x} = 0$. Then the corresponding variational problem of (4.1) is given as follows:

Proposition 4.1. *Seek* $\boldsymbol{u} \in [H_0^1(\Omega)]^d$, $p \in L_0^2(\Omega)$ *satisfying*

$$2\mu(\varepsilon(\boldsymbol{u}), \varepsilon(\boldsymbol{v})) + (\nabla \cdot \boldsymbol{v}, p) = (\boldsymbol{f}, \boldsymbol{v}), \tag{4.2a}$$

$$(\nabla \cdot \boldsymbol{u}, q) - \lambda^{-1}(p, q) = 0, \tag{4.2b}$$

for all $\boldsymbol{v} \in [H_0^1(\Omega)]^d$ *and* $q \in L_0^2(\Omega)$.

Assume that the generalized Stokes Eqs. (4.1) possesses the $H^{s+1}(\Omega) \times H^s(\Omega)$-regularity [44,45], i.e.

$$\|\boldsymbol{u}\|_{s+1} + \|p\|_s \le C\|\boldsymbol{f}\|_{s-1}, \tag{4.3}$$

where $s \in (\frac{1}{2}, 1]$, C is a constant independent of λ.

4.1. Mixed scheme

Given the introduction of the auxiliary variable p within the mixed formulation (4.5), defining an additional finite element space becomes necessary. More precisely, we denote

$$W_h := \{q \in L_0^2(\Omega) : q|_T \in P_{k-1}(T),\ \forall T \in \mathcal{T}_h\},$$

and following bilinear forms

$$a(\boldsymbol{v}, \boldsymbol{w}) := 2\mu(\varepsilon_w(\boldsymbol{v}), \varepsilon_w(\boldsymbol{w})) = \sum_{T\in\mathcal{T}_h} 2\mu(\varepsilon_w(\boldsymbol{v}), \varepsilon_w(\boldsymbol{w}))_T, \tag{4.4a}$$

$$b(\boldsymbol{v}, q) := (\nabla_w \cdot \boldsymbol{v}, q) = \sum_{T\in\mathcal{T}_h} (\nabla_w \cdot \boldsymbol{v}, q)_T, \tag{4.4b}$$

$$d(q, r) := \lambda^{-1}(q, r) = \sum_{T\in\mathcal{T}_h} \lambda^{-1}(q, r)_T, \tag{4.4c}$$

where $\boldsymbol{v}, \boldsymbol{w} \in V_h$, $q, r \in W_h$.

Now we are ready to propose the mixed CDG scheme for the elasticity problems:

Weak Galerkin Algorithm 2. *For a numerical solution of (4.2), seeking $(\boldsymbol{u}_h, p_h) \in V_h \times W_h$ satisfying*

$$a(\boldsymbol{u}_h, \boldsymbol{v}) + b(\boldsymbol{v}, p_h) = (\boldsymbol{f}, \boldsymbol{v}), \qquad \forall \boldsymbol{v} \in V_h, \tag{4.5a}$$

$$b(\boldsymbol{u}_h, q) - d(p_h, q) = 0, \qquad \forall q \in W_h. \tag{4.5b}$$

Theorem 4.2. *The solutions of primal scheme (3.3) and mixed scheme (4.5) are equivalent. More specially, the solution $\boldsymbol{u}_h$ for (3.3) and (4.5) are identical.*

Proof. Suppose $(\boldsymbol{u}_h, p_h)$ is the solution of (4.5), we have

$$(\nabla_w \cdot \boldsymbol{u}_h, q)_T - \lambda^{-1}(p_h, q)_T = 0, \qquad \forall q \in P_{k-1}(T).$$

By using (4.5b) yields

$$\nabla_w \cdot \boldsymbol{u}_h = \lambda^{-1} p_h, \tag{4.6}$$

where we have used the fact that $\nabla_w \cdot \boldsymbol{u}_h \in P_{k-1}(T)$. Substituting (4.6) into (4.5a), we get

$$\mathcal{A}(\boldsymbol{u}_h, \boldsymbol{v}) = a(\boldsymbol{u}_h, \boldsymbol{v}) + b(\boldsymbol{v}, \lambda\nabla_w \cdot \boldsymbol{u}_h) = (\boldsymbol{f}, \boldsymbol{v}), \qquad \forall \boldsymbol{v} \in V_h. \tag{4.7}$$

According to the existence and uniqueness of the numerical solution, it follows that $\boldsymbol{u}_h$ is also the solution of (3.3).

For another direction, suppose $\boldsymbol{u}_h$ solves (3.3) and denote $p_h = \lambda\nabla_w \cdot \boldsymbol{u}_h$, one can get (4.5) immediately, i.e. solutions of (3.3) and (4.5) are equivalent. $\square$

The formulation (4.2) of elasticity problems, modeled as a generalized Stokes system, frequently yields numerical approximations that remain locking-free as λ approaches infinity. Since the solutions of both the primal CDG scheme (3.3) and the mixed CDG scheme (4.5) are equivalent, the locking-free behavior of (3.3) is established when it can be demonstrated that the error estimate for the mixed CDG scheme (4.5) applied to (4.2) is λ-independent.

4.2. Stability condition

Introducing the following semi-norms on V_h by

$$|||\boldsymbol{v}|||^2 := 2\mu(\varepsilon_w(\boldsymbol{v}), \varepsilon_w(\boldsymbol{v})),$$

$$\|\boldsymbol{v}\|_{1,h}^2 := \sum_{T\in\mathcal{T}_h} \|\varepsilon(\boldsymbol{v})\|_T^2 + \sum_{e\in\mathcal{E}_h} h_e^{-1}\|\boldsymbol{v} - \{\boldsymbol{v}\}\|_e^2.$$

It is easy to see that $\|\cdot\|_{1,h}$ also defines a norm on V_h and following the similar procedure as the Lemma 3.2 in [25], we have

$$C_1\|\boldsymbol{v}\|_{1,h} \le |||\boldsymbol{v}||| \le C_2\|\boldsymbol{v}\|_{1,h}. \tag{4.8}$$

Therefore, by summing up (3.6) over all elements, we have

Lemma 4.1. $|||\cdot|||$ *is a norm on V_h and*

$$|||\boldsymbol{v}|||^2 \ge C \sum_{T\in\mathcal{T}_h} h_T^{-1}\|\boldsymbol{v} - \{\boldsymbol{v}\}\|_{\partial T}^2. \tag{4.9}$$

To establish the energy estimate, we introduce the following inf-sup condition:

Lemma 4.2 (*inf-sup Condition, [43,46]*). *There exists a constant $\beta > 0$ such that*

$$\sup_{\boldsymbol{v}\in V_h^0,\boldsymbol{v}\neq 0} \frac{b(\boldsymbol{v},q)}{|||\boldsymbol{v}|||} \geq \beta\|q\|, \qquad \forall q \in W_h. \tag{4.10}$$

5. Preparation for error analysis

In this section, we prepare for the subsequent error analysis by deriving the error equations and some related inequalities.

For $T \in \mathcal{T}_h$, Q_h denotes the L^2 projection onto $[P_k(T)]^d$. Let $\boldsymbol{Q}_h$ represent the L^2 projection onto $[P_j(T)]^{d\times d}$ $(j = n + k - 1)$, and $\mathbb{Q}_h$ be the L^2 projection onto $P_{k-1}(T)$.

Lemma 5.1. *Suppose $\boldsymbol{Q}_h$ and $\mathbb{Q}_h$ are projection operators, then*

$$\nabla_w \boldsymbol{v} = \boldsymbol{Q}_h(\nabla \boldsymbol{v}), \tag{5.1}$$

$$\nabla_w \cdot \boldsymbol{v} = \mathbb{Q}_h(\nabla \cdot \boldsymbol{v}), \tag{5.2}$$

for any $\boldsymbol{v} \in [H^1(\Omega)]^d$.

Proof. We only present a proof of (5.1). A similar approach can be adapted to (5.2). For any $\varphi \in [P_j(T)]^{d\times d}$, by using the definition of discrete weak gradient, integration by parts, and the definition of $\boldsymbol{Q}_h$, we arrive at

$$\begin{aligned}
(\nabla_w \boldsymbol{v}, \varphi)_T &= -(\boldsymbol{v}, \nabla\cdot\varphi)_T + \langle\{\boldsymbol{v}\}, \varphi\cdot\boldsymbol{n}\rangle_{\partial T}\\
&= -(\boldsymbol{v}, \nabla\cdot\varphi)_T + \langle\boldsymbol{v}, \varphi\cdot\boldsymbol{n}\rangle_{\partial T}\\
&= (\nabla\boldsymbol{v}, \varphi)_T = (\boldsymbol{Q}_h(\nabla\boldsymbol{v}), \varphi)_T.
\end{aligned}$$

The proof is completed. □

Corollary. *For all $\boldsymbol{v} \in [H^1(\Omega)]^d$, there holds*

$$\varepsilon_w(\boldsymbol{v}) = \boldsymbol{Q}_h\varepsilon(\boldsymbol{v}). \tag{5.3}$$

Suppose $(\boldsymbol{u}, p)$ solves (4.1), $(\boldsymbol{u}_h, p_h)$ is the solution of (4.5), denotes the corresponding error functions by $\boldsymbol{e}_h = \boldsymbol{u} - \boldsymbol{u}_h$, $\xi_h = \mathbb{Q}_h p - p_h$.

Lemma 5.2 (*Error equations*). *For any $\boldsymbol{v} \in V_h, q_h \in W_h$, we have the following error equations:*

$$a(\boldsymbol{e}_h, \boldsymbol{v}) + b(\boldsymbol{v}, \xi_h) = l(\boldsymbol{u}, \boldsymbol{v}) + \theta(p, \boldsymbol{v}), \tag{5.4a}$$

$$b(\boldsymbol{e}_h, q_h) - d(\xi_h, q_h) = 0, \tag{5.4b}$$

where

$$\begin{aligned}
l(\boldsymbol{u}, \boldsymbol{v}) &= \sum_{T\in\mathcal{T}_h} \langle \boldsymbol{v} - \{\boldsymbol{v}\}, 2\mu(\varepsilon(\boldsymbol{u}) - \boldsymbol{Q}_h\varepsilon(\boldsymbol{u}))\cdot\boldsymbol{n}\rangle_{\partial T},\\
\theta(p, \boldsymbol{v}) &= \sum_{T\in\mathcal{T}_h} \langle \boldsymbol{v} - \{\boldsymbol{v}\}, (p - \mathbb{Q}_h p)\boldsymbol{n}\rangle_{\partial T}.
\end{aligned}$$

Proof. Choosing $\boldsymbol{v} \in V_h$ as a test function in (4.1a) and using integration by parts, we get

$$\begin{aligned}
-(\nabla\cdot\varepsilon(\boldsymbol{u}), \boldsymbol{v}) &= \sum_{T\in\mathcal{T}_h} (\varepsilon(\boldsymbol{u}), \nabla\boldsymbol{v})_T - \sum_{T\in\mathcal{T}_h} \langle\boldsymbol{v}, \varepsilon(\boldsymbol{u})\cdot\boldsymbol{n}\rangle_{\partial T}\\
&= \sum_{T\in\mathcal{T}_h} (\nabla\boldsymbol{v}, \boldsymbol{Q}_h\varepsilon(\boldsymbol{u}))_T - \sum_{T\in\mathcal{T}_h} \langle\boldsymbol{v} - \{\boldsymbol{v}\}, \varepsilon(\boldsymbol{u})\cdot\boldsymbol{n}\rangle_{\partial T}\\
&= -\sum_{T\in\mathcal{T}_h} (\boldsymbol{v}, \nabla\cdot(\boldsymbol{Q}_h\varepsilon(\boldsymbol{u})))_T + \sum_{T\in\mathcal{T}_h} \langle\boldsymbol{v} - \{\boldsymbol{v}\}, \boldsymbol{Q}_h\varepsilon(\boldsymbol{u})\cdot\boldsymbol{n}\rangle_{\partial T}\\
&\quad + \sum_{T\in\mathcal{T}_h} \langle\{\boldsymbol{v}\}, \boldsymbol{Q}_h\varepsilon(\boldsymbol{u})\cdot\boldsymbol{n}\rangle_{\partial T} - \sum_{T\in\mathcal{T}_h} \langle\boldsymbol{v} - \{\boldsymbol{v}\}, \varepsilon(\boldsymbol{u})\cdot\boldsymbol{n}\rangle_{\partial T},
\end{aligned} \tag{5.5}$$

and

$$\begin{aligned}
-(\nabla p, \boldsymbol{v}) &= \sum_{T\in\mathcal{T}_h} (p, \nabla\cdot\boldsymbol{v})_T - \sum_{T\in\mathcal{T}_h} \langle\boldsymbol{v}, p\boldsymbol{n}\rangle_{\partial T}\\
&= \sum_{T\in\mathcal{T}_h} (\nabla\cdot\boldsymbol{v}, \mathbb{Q}_h p)_T - \sum_{T\in\mathcal{T}_h} \langle\boldsymbol{v} - \{\boldsymbol{v}\}, p\boldsymbol{n}\rangle_{\partial T}\\
&= -\sum_{T\in\mathcal{T}_h} (\boldsymbol{v}, \nabla(\mathbb{Q}_h p))_T + \sum_{T\in\mathcal{T}_h} \langle\boldsymbol{v} - \{\boldsymbol{v}\}, (\mathbb{Q}_h p)\boldsymbol{n}\rangle_{\partial T}\\
&\quad + \sum_{T\in\mathcal{T}_h} \langle\{\boldsymbol{v}\}, (\mathbb{Q}_h p)\boldsymbol{n}\rangle_{\partial T} - \sum_{T\in\mathcal{T}_h} \langle\boldsymbol{v} - \{\boldsymbol{v}\}, p\boldsymbol{n}\rangle_{\partial T},
\end{aligned} \tag{5.6}$$

here we have used the facts that $\sum_{T\in\mathcal{T}_h}\langle\{\boldsymbol{v}\},\nabla\boldsymbol{u}\cdot\boldsymbol{n}\rangle=0$ and $\sum_{T\in\mathcal{T}_h}\langle\{\boldsymbol{v}\},p\boldsymbol{n}\rangle=0$. From the definitions of discrete weak gradient and weak divergence, we arrive at

$$-(\nabla\cdot\varepsilon(\boldsymbol{u}),\boldsymbol{v})=\sum_{T\in\mathcal{T}_h}(\varepsilon_w(\boldsymbol{v}),\boldsymbol{Q}_h\varepsilon(\boldsymbol{u}))_T+\sum_{T\in\mathcal{T}_h}\langle\boldsymbol{v}-\{\boldsymbol{v}\},\left(\boldsymbol{Q}_h\varepsilon(\boldsymbol{u})-\varepsilon(\boldsymbol{u})\right)\cdot\boldsymbol{n}\rangle_{\partial T},\tag{5.7}$$

and

$$-(\nabla p,\boldsymbol{v})=\sum_{T\in\mathcal{T}_h}(\nabla_w\cdot\boldsymbol{v},\mathbb{Q}_hp)_T+\sum_{T\in\mathcal{T}_h}\langle\boldsymbol{v}-\{\boldsymbol{v}\},(\mathbb{Q}_hp-p)\boldsymbol{n}\rangle_{\partial T}.\tag{5.8}$$

Combining (5.7)–(5.8), it follows that

$$\begin{aligned}a(\boldsymbol{u}_h,\boldsymbol{v})+b(\boldsymbol{v},p_h)&=(\boldsymbol{f},\boldsymbol{v})\\&=a(\boldsymbol{u},\boldsymbol{v})+b(\boldsymbol{v},\mathbb{Q}_hp)-l(\boldsymbol{u},\boldsymbol{v})-\theta(p,\boldsymbol{v}),\end{aligned}\tag{5.9}$$

which yields (5.4a).

As for (5.4b), taking $q_h\in W_h$ as the test function in (4.1b), we get

$$0=(\nabla\cdot\boldsymbol{u},q_h)-\lambda^{-1}(p,\boldsymbol{q}_h)=(\nabla_w\cdot\boldsymbol{u},q_h)-\lambda^{-1}(\mathbb{Q}_hp,q_h),\tag{5.10}$$

then we can deduce (5.4b) by minusing (4.5b). □

Before proving the error estimates, we establish the following inequality estimate results.

Lemma 5.3. *For any $\boldsymbol{w}\in[H^{k+1}(\Omega)]^d,\rho\in H^k(\Omega)$, and $\boldsymbol{v}\in V_h$, we have*

$$|l(\boldsymbol{w},\boldsymbol{v})|\le Ch^k\|\boldsymbol{w}\|_{k+1}\,|||\,\boldsymbol{v}|||,\tag{5.11a}$$

$$|\theta(\rho,\boldsymbol{v})|\le Ch^k\|\rho\|_k\,|||\,\boldsymbol{v}\,|||\,.\tag{5.11b}$$

Lemma 5.4. *For any $\boldsymbol{w}\in[H^{k+1}(\Omega)]^d$, there holds*

$$|||\boldsymbol{w}-Q_h\boldsymbol{w}|||\le Ch^k\|\boldsymbol{w}\|_{k+1}.\tag{5.12}$$

Lemma 5.5. *For any $\boldsymbol{w}\in[H^{k+1}(\Omega)]^d$ and $q\in W_h$, we have*

$$(\nabla\cdot\boldsymbol{w},q)=(\nabla_w\cdot Q_h\boldsymbol{w},q)+\chi(\boldsymbol{w},q),\tag{5.13}$$

and

$$|\chi(\boldsymbol{w},q)|\le Ch^k\|\boldsymbol{w}\|_{k+1}\|q\|,\tag{5.14}$$

where

$$\chi(\boldsymbol{w},q)=\sum_{T\in\mathcal{T}_h}\langle\{\boldsymbol{w}-Q_h\boldsymbol{w}\}\cdot\boldsymbol{n},q\rangle_{\partial T}.$$

For the proofs of the above lemmas, see Appendices A.1, A.2, A.3 for details.

6. Error estimate in a discrete H^1-norm

In this section, we establish an error estimate in the H^1-norm for the CDG finite element approximation $(\boldsymbol{u}_h,p_h)$.

Theorem 6.1 (*Energy Estimate*). *Let $(\boldsymbol{u},p)\in[H^{k+1}(\Omega)]^d\times H^k(\Omega)\,(k\ge1)$ represent the exact solution to (4.1) and denote $(\boldsymbol{u}_h,p_h)\in V_h\times W_h$ as the numerical solution derived from the CDG scheme (4.5). $\boldsymbol{e}_h=\boldsymbol{u}-\boldsymbol{u}_h$ and $\xi_h=\mathbb{Q}_hp-p_h$ are the error functions, then we can acquire the ensuing error estimate:*

$$|||\,\boldsymbol{e}_h\,|||+\lambda^{-1/2}\|\xi_h\|\le Ch^k(\|\boldsymbol{u}\|_{k+1}+\|p\|_k),\tag{6.1}$$

where positive constant C independent of λ and mesh size h.

Proof. Denotes $\boldsymbol{\rho}_h=Q_h\boldsymbol{u}-\boldsymbol{u}_h$, then we get

$$\begin{aligned}|||\boldsymbol{e}_h|||^2&=2\mu(\varepsilon_w(\boldsymbol{e}_h),\varepsilon_w(\boldsymbol{e}_h))\\&=2\mu(\varepsilon_w(\boldsymbol{e}_h),\varepsilon_w(\boldsymbol{u}-Q_h\boldsymbol{u}))+2\mu(\varepsilon_w(\boldsymbol{e}_h),\varepsilon_w(\boldsymbol{\rho}_h)).\end{aligned}\tag{6.2}$$

Letting $\boldsymbol{v}=\boldsymbol{\rho}_h$ in (5.4a) and $q_h=\xi_h$ in (5.4b), we have

$$a(\boldsymbol{e}_h,\boldsymbol{\rho}_h)+b(\boldsymbol{\rho}_h,\xi_h)=l(\boldsymbol{u},\boldsymbol{\rho}_h)+\theta(p,\boldsymbol{\rho}_h),\tag{6.3}$$

and

$$\begin{aligned} d(\xi_h,\xi_h) &= b(\boldsymbol{e}_h,\xi_h) \\ &= (\nabla_w\cdot(\boldsymbol{u}-\boldsymbol{u}_h),\xi_h) \\ &= (\nabla_w\cdot\boldsymbol{u},\xi_h)-(\nabla_w\cdot\boldsymbol{u}_h,\xi_h) \\ &= (\nabla_w\cdot(\boldsymbol{u}-Q_h\boldsymbol{u}),\xi_h)+(\nabla_w\cdot\boldsymbol{\rho}_h,\xi_h) \\ &= (\nabla_w\cdot\boldsymbol{u},\xi_h)-(\nabla_w\cdot Q_h\boldsymbol{u},\xi_h)+b(\boldsymbol{\rho}_h,\xi_h) \\ &= (\nabla\cdot\boldsymbol{u},\xi_h)-(\nabla_w\cdot Q_h\boldsymbol{u},\xi_h)+b(\boldsymbol{\rho}_h,\xi_h) \\ &= b(\boldsymbol{\rho}_h,\xi_h)+\chi(\boldsymbol{u},\xi_h), \end{aligned} \tag{6.4}$$

where we have used Lemma 5.5 in (6.4). Substituting (6.4) into (6.3) yields

$$a(\boldsymbol{e}_h,\boldsymbol{\rho}_h)+d(\xi_h,\xi_h)=l(\boldsymbol{u},\boldsymbol{\rho}_h)+\theta(p,\boldsymbol{\rho}_h)+\chi(\boldsymbol{u},\xi_h). \tag{6.5}$$

Combining (6.2) and (6.5), we deduce

$$|||\,\boldsymbol{e}_h\,|||^2+\lambda^{-1}\|\xi_h\|^2=2\mu(\varepsilon_w(\boldsymbol{e}_h),\varepsilon_w(\boldsymbol{u}-Q_h\boldsymbol{u}))+l(\boldsymbol{u},\boldsymbol{\rho}_h)+\theta(p,\boldsymbol{\rho}_h)+\chi(\boldsymbol{u},\xi_h). \tag{6.6}$$

By using Lemma 5.4 and Young's inequality, we obtain

$$\begin{aligned} \left|\sum_{T\in\mathcal{T}_h}2\mu(\varepsilon_w(\boldsymbol{e}_h),\varepsilon_w(\boldsymbol{u}-Q_h\boldsymbol{u}))_T\right| &\le C\,|||\,\boldsymbol{e}_h\,|||\;|||\boldsymbol{u}-Q_h\boldsymbol{u}||| \\ &\le Ch^{2k}\|\boldsymbol{u}\|_{k+1}^2+\frac{1}{4}\,|||\,\boldsymbol{e}_h\,|||^2\,. \end{aligned} \tag{6.7}$$

From the error equation (5.4a) and Lemma 5.3, it follows that

$$\begin{aligned} |b(\boldsymbol{v},\xi_h)| &= \left|l(\boldsymbol{u},\boldsymbol{v})+\theta(p,\boldsymbol{v})-a(\boldsymbol{e}_h,\boldsymbol{v})\right| \\ &\le Ch^k(\|\boldsymbol{u}\|_{k+1}+\|p\|_k)\,|||\,\boldsymbol{v}\,|||+C\,|||\,\boldsymbol{e}_h\,|||\;|||\boldsymbol{v}|||, \end{aligned}$$

then by the inf-sup condition (4.10), we get

$$\|\xi_h\|\le\beta^{-1}\sup\frac{b(\boldsymbol{v},\xi_h)}{|||\boldsymbol{v}|||}\le Ch^k(\|\boldsymbol{u}\|_{k+1}+\|p\|_k)+C\,|||\,\boldsymbol{e}_h\,|||\,.$$

Therefore, by using Lemmas 5.3, 5.5, and Young's inequality, it follows that

$$\begin{aligned} |l(\boldsymbol{u},\boldsymbol{\rho}_h)+\theta(p,\boldsymbol{\rho}_h)+\chi(\boldsymbol{u},\xi_h)| &\le |l(\boldsymbol{u},\boldsymbol{\rho}_h)|+|\theta(p,\boldsymbol{\rho}_h)|+|\chi(\boldsymbol{u},\xi_h)| \\ &\le Ch^k(\|\boldsymbol{u}\|_{k+1}+\|p\|_k)\,|||\,\boldsymbol{\rho}_h\,|||+Ch^k\|\boldsymbol{u}\|_{k+1}\|\xi_h\| \\ &\le Ch^k(\|\boldsymbol{u}\|_{k+1}+\|p\|_k)\left(|||\boldsymbol{u}-Q_h\boldsymbol{u}\,|||+|||\,\boldsymbol{e}_h|||\right) \\ &\quad+Ch^{2k}(\|\boldsymbol{u}\|_{k+1}+\|p\|_k)^2+Ch^k(\|\boldsymbol{u}\|_{k+1}+\|p\|_k)\,|||\,\boldsymbol{e}_h||| \\ &\le Ch^{2k}(\|\boldsymbol{u}\|_{k+1}+\|p\|_k)^2+Ch^k(\|\boldsymbol{u}\|_{k+1}+\|p\|_k)\,|||\,\boldsymbol{e}_h||| \\ &\le Ch^{2k}(\|\boldsymbol{u}\|_{k+1}+\|p\|_k)^2+\frac{1}{4}\,|||\,\boldsymbol{e}_h|||^2, \end{aligned}$$

which leads to

$$|||\boldsymbol{e}_h|||\le Ch^k(\|\boldsymbol{u}\|_{k+1}+\|p\|_k), \tag{6.8}$$

thus

$$|||\,\boldsymbol{e}_h\,|||^2+\lambda^{-1}\|\xi_h\|^2\le Ch^{2k}(\|\boldsymbol{u}\|_{k+1}+\|p\|_k)^2, \tag{6.9}$$

i.e., the desired inequality is obtained. □

7. Error estimate in L^2-norm

In this section, we are going to use the standard duality argument to obtain an L^2 estimate for the CDG method. Recall $\boldsymbol{e}_h=\boldsymbol{u}-\boldsymbol{u}_h$ and denote $\boldsymbol{\rho}_h=Q_h\boldsymbol{u}-\boldsymbol{u}_h$, the following dual problem is considered:

Proposition 7.1. *Seek* $(\boldsymbol{\psi},\phi)\in[H^2(\Omega)]^d\times H^1(\Omega)$ *satisfying*

$$-\nabla\cdot(2\mu\varepsilon(\boldsymbol{\psi}))-\nabla\phi=\boldsymbol{\rho}_h,\qquad \text{in } \Omega, \tag{7.1a}$$

$$\nabla\cdot\boldsymbol{\psi}=\lambda^{-1}\phi,\qquad \text{in } \Omega, \tag{7.1b}$$

$$\boldsymbol{\psi}=\boldsymbol{0},\qquad \text{on } \partial\Omega. \tag{7.1c}$$

Suppose that (7.1) possesses the $[H^2(\Omega)]^d \times H^1(\Omega)$-regularity estimate, i.e.

$$\|\boldsymbol{\psi}\|_2 + \|\phi\|_1 \le C\|\boldsymbol{\rho}_h\|. \tag{7.2}$$

Theorem 7.2 (L^2-estimate). *Let $(\boldsymbol{u}, p) \in [H^{k+1}(\Omega)]^d \times H^k(\Omega)$ represent the exact solution of (4.1), and denote the numerical solution of the CDG scheme (4.5) as $(\boldsymbol{u}_h, p_h) \in V_h \times W_h$. Define the error functions as $\boldsymbol{e}_h = \boldsymbol{u} - \boldsymbol{u}_h$ and $\xi_h = \mathbb{Q}_h p - p_h$. We can then establish the following error estimate:*

$$\|\boldsymbol{e}_h\| \le Ch^{k+1}(\|\boldsymbol{u}\|_{k+1} + \|p\|_k), \tag{7.3}$$

where constant $C > 0$ is independent of λ and mesh size h.

Proof. Testing (7.1) with $\boldsymbol{\rho}_h$, we have

$$\begin{aligned}\|\boldsymbol{\rho}_h\|^2 &= (\boldsymbol{\rho}_h, \boldsymbol{\rho}_h) = -(\nabla\cdot(2\mu\varepsilon(\boldsymbol{\psi})), \boldsymbol{\rho}_h) - (\nabla\phi, \boldsymbol{\rho}_h)\\ &= a(\boldsymbol{\psi}, \boldsymbol{\rho}_h) + b(\boldsymbol{\rho}_h, \mathbb{Q}_h\phi) - l(\boldsymbol{\psi}, \boldsymbol{\rho}_h) - \theta(\phi, \boldsymbol{\rho}_h).\end{aligned} \tag{7.4}$$

According to the error equation (5.4b) and Lemma 5.5, we obtain

$$\begin{aligned} d(\xi_h, q_h) &= b(\boldsymbol{e}_h, q_h)\\ &= (\nabla_w\cdot(\boldsymbol{u}-\boldsymbol{u}_h), q_h)\\ &= (\nabla_w\cdot\boldsymbol{u}, q_h) - (\nabla_w\cdot\boldsymbol{u}_h, q_h)\\ &= (\nabla_w\cdot(\boldsymbol{u}-Q_h\boldsymbol{u}), q_h) + (\nabla_w\cdot\boldsymbol{\rho}_h, q_h)\\ &= (\nabla_w\cdot\boldsymbol{u}, q_h) - (\nabla_w\cdot Q_h\boldsymbol{u}, q_h) + b(\boldsymbol{\rho}_h, q_h)\\ &= b(\boldsymbol{\rho}_h, q_h) + \chi(\boldsymbol{u}, q_h), \ \ \forall q_h \in W_h.\end{aligned} \tag{7.5}$$

From Lemma 5.5, (5.2), and (7.1b) yields

$$\begin{aligned} b(Q_h\boldsymbol{\psi}, \xi_h) &= b(\boldsymbol{\psi}, \xi_h) - \chi(\boldsymbol{\psi}, \xi_h)\\ &= (\nabla_w\cdot\boldsymbol{\psi}, \xi_h) - \chi(\boldsymbol{\psi}, \xi_h)\\ &= (\mathbb{Q}_h(\nabla\cdot\boldsymbol{\psi}), \xi_h) - \chi(\boldsymbol{\psi}, \xi_h)\\ &= (\lambda^{-1}\mathbb{Q}_h\phi, \xi_h) - \chi(\boldsymbol{\psi}, \xi_h)\\ &= d(\mathbb{Q}_h\phi, \xi_h) - \chi(\boldsymbol{\psi}, \xi_h).\end{aligned} \tag{7.6}$$

Therefore, by taking $q_h = \mathbb{Q}_h\phi$ in (7.5) gives

$$\begin{aligned} b(Q_h\boldsymbol{\psi}, \xi_h) &= d(\mathbb{Q}_h\phi, \xi_h) - \chi(\boldsymbol{\psi}, \xi_h)\\ &= b(\boldsymbol{\rho}_h, \mathbb{Q}_h\phi) + \chi(\boldsymbol{u}, \mathbb{Q}_h\phi) - \chi(\boldsymbol{\psi}, \xi_h).\end{aligned} \tag{7.7}$$

Thus, combining the above equations, we derive

$$\begin{aligned}\|\boldsymbol{\rho}_h\|^2 &= a(\boldsymbol{\psi}, \boldsymbol{\rho}_h) + b(Q_h\boldsymbol{\psi}, \xi_h) - l(\boldsymbol{\psi}, \boldsymbol{\rho}_h) - \theta(\phi, \boldsymbol{\rho}_h) - \chi(\boldsymbol{u}, \mathbb{Q}_h\phi) + \chi(\boldsymbol{\psi}, \xi_h)\\ &= a(\boldsymbol{e}_h, \boldsymbol{\psi}) + a(Q_h\boldsymbol{u}-\boldsymbol{u}, \boldsymbol{\psi}) + b(Q_h\boldsymbol{\psi}, \xi_h) - l(\boldsymbol{\psi}, \boldsymbol{\rho}_h) - \theta(\phi, \boldsymbol{\rho}_h)\\ &\quad - \chi(\boldsymbol{u}, \mathbb{Q}_h\phi) + \chi(\boldsymbol{\psi}, \xi_h)\\ &= a(Q_h\boldsymbol{u}-\boldsymbol{u}, \boldsymbol{\psi}) + a(\boldsymbol{e}_h, \boldsymbol{\psi}-Q_h\boldsymbol{\psi}) + a(\boldsymbol{e}_h, Q_h\boldsymbol{\psi}) + b(Q_h\boldsymbol{\psi}, \xi_h) - l(\boldsymbol{\psi}, \boldsymbol{\rho}_h) - \theta(\phi, \boldsymbol{\rho}_h)\\ &\quad - \chi(\boldsymbol{u}, \mathbb{Q}_h\phi) + \chi(\boldsymbol{\psi}, \xi_h)\\ &= a(Q_h\boldsymbol{u}-\boldsymbol{u}, \boldsymbol{\psi}) + a(\boldsymbol{e}_h, \boldsymbol{\psi}-Q_h\boldsymbol{\psi}) + l(\boldsymbol{u}, Q_h\boldsymbol{\psi}) + \theta(p, Q_h\boldsymbol{\psi}) - l(\boldsymbol{\psi}, \boldsymbol{\rho}_h) - \theta(\phi, \boldsymbol{\rho}_h)\\ &\quad - \chi(\boldsymbol{u}, \mathbb{Q}_h\phi) + \chi(\boldsymbol{\psi}, \xi_h)\\ &:= I_1 + I_2 + I_3 + I_4 + I_5 + I_6 + I_7 + I_8.\end{aligned} \tag{7.8}$$

By Lemma A.4 and regularity (7.2), it follows that

$$\begin{aligned}\|\boldsymbol{\rho}_h\|^2 &\le Ch^{k+1}(\|\boldsymbol{u}\|_{k+1} + \|p\|_k)(\|\boldsymbol{\psi}\|_2 + \|\phi\|_1)\\ &\le Ch^{k+1}(\|\boldsymbol{u}\|_{k+1} + \|p\|_k)\|\boldsymbol{\rho}_h\|,\end{aligned}$$

i.e.

$$\|\boldsymbol{\rho}_h\| \le Ch^{k+1}(\|\boldsymbol{u}\|_{k+1} + \|p\|_k). \tag{7.9}$$

Hence, using the triangle inequality and projection inequality, we arrive at

$$\|\boldsymbol{e}_h\| \le \|\boldsymbol{\rho}_h\| + \|\boldsymbol{u} - Q_h\boldsymbol{u}\| \le Ch^{k+1}(\|\boldsymbol{u}\|_{k+1} + \|p\|_k). \tag{7.10}$$

This completes the proof of the theorem. □

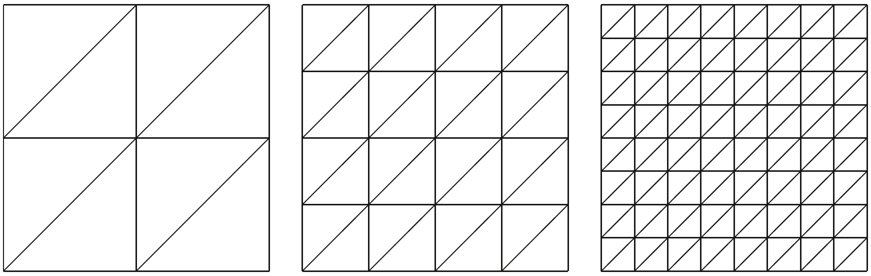

Fig. 1. The uniform triangular grids with $h = \frac{1}{2}, \frac{1}{4}, \frac{1}{8}$.

Theorem 7.3. *Let σ be the stress tensor, σ_h be the approximate stress tensor, there holds*

$$\|\sigma - \sigma_h\| \le Ch^k(\|\boldsymbol{u}\|_{k+1} + \|p\|_k), \tag{7.11}$$

where $\sigma_h = 2\mu\varepsilon_w(\boldsymbol{u}_h) + \lambda(\nabla_w \cdot \boldsymbol{u_h})\mathbb{I}$.

Proof. According to (4.1) and the equivalence between the two CDG methods in Theorem 4.2, we have

$$\sigma = 2\mu\varepsilon(\boldsymbol{u}) + p\mathbb{I}, \quad \sigma_h = 2\mu\varepsilon_w(\boldsymbol{u}_h) + p_h\mathbb{I}.$$

By using the triangle inequality, projection inequality, and Theorem 6.1, we get

$$\begin{aligned}\|\sigma - \sigma_h\| \le& 2\mu\|\varepsilon(\boldsymbol{u}) - \varepsilon_w(\boldsymbol{u}_h)\| + C\|p - p_h\| \\ \le& ||| \boldsymbol{u} - \boldsymbol{u}_h ||| + C\|p - \mathbb{Q}_h p\| + C\|\mathbb{Q}_h p - p_h\| \\ \le& Ch^k(\|\boldsymbol{u}\|_{k+1} + \|p\|_k),\end{aligned}$$

which concludes the proof. □

8. Numerical results

In this section, we present numerical examples to validate the accuracy and locking-free property of the CDG scheme (3.3). In the numerical examples, we have introduced polygonal meshes (Fig. 4) and deformed meshes (Fig. 3) in addition to the conventional triangular meshes (Fig. 1) and rectangular meshes (Fig. 2). Notably, the procedural generation of the polygonal meshes is achieved by utilizing the FEALPy package [47].

8.1. Accuracy test

Example 8.1. Consider the elasticity problems (1.1) in domain $\Omega = (0,1) \times (0,1)$ with the exact solution

$$\boldsymbol{u} = \begin{pmatrix} \sin(\pi x)\sin(\pi y) \\ \sin(\pi x)\sin(\pi y) \end{pmatrix},$$

and the right-hand side function $\boldsymbol{f}$ is

$$\boldsymbol{f} = -\mu\begin{pmatrix} -2\pi^2\sin(\pi x)\sin(\pi y) \\ -2\pi^2\sin(\pi x)\sin(\pi y) \end{pmatrix} - (\lambda+\mu)\begin{pmatrix} -\pi^2\sin(\pi x)\sin(\pi y) + \pi^2\cos(\pi x)\cos(\pi y) \\ -\pi^2\sin(\pi x)\sin(\pi y) + \pi^2\cos(\pi x)\cos(\pi y) \end{pmatrix}.$$

In this example, we set $\mu = 1$ and $\lambda = 1$.

Firstly, we compute in a uniform triangular grid as shown in Fig. 1. In the numerical computation, the weak gradient operator ∇_w is obtained from the $[P_{k+2}]^{2\times 2}$ polynomial space. Table 1 lists the corresponding error and convergence order.

Then, we use uniform rectangular grids (Fig. 2) and deformed rectangular grids (Fig. 3) for computation. The weak gradient operator ∇_w is derived through the polynomial space $[P_{k+3}]^{2\times 2}$ in the numerical computation. The numerical results are shown in Tables 2–3.

Finally, we use the polygonal grids as shown in Fig. 4 to solve this numerical example. In the numerical computation, the weak gradient operator ∇_w is computed in the $[P_{k+5}]^{2\times 2}$ polynomial space. We list the results of the computation in Table 4.

In the preceding theoretical exposition, the optimal convergence rates for the H^1-norm and L^2-norm are established as $O(h^k)$ and $O(h^{k+1})$, respectively. From Tables 1–4, it can be seen that all convergence rates have reached the optimal order, which is consistent with our theoretical analysis.

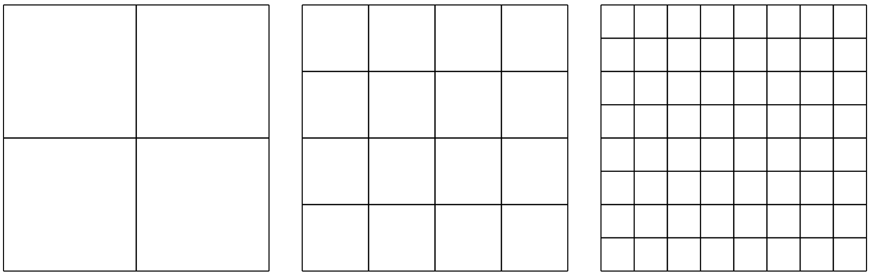

Fig. 2. The uniform rectangular grids with $h = \frac{1}{2}, \frac{1}{4}, \frac{1}{8}$.

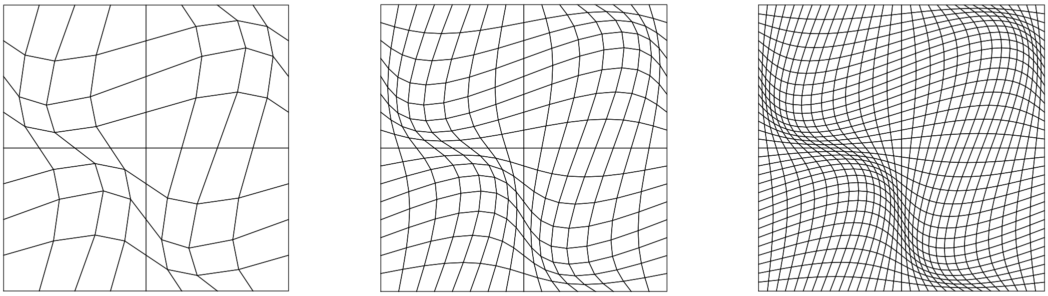

Fig. 3. The deformed rectangular grids with $h = \frac{1}{8}, \frac{1}{16}, \frac{1}{32}$.

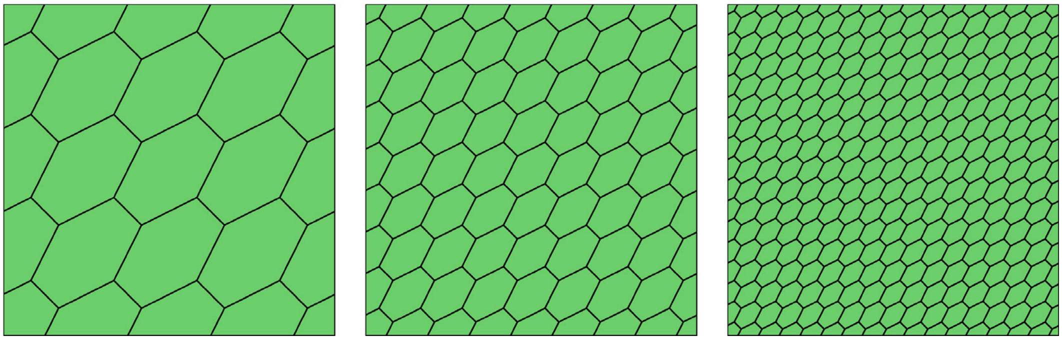

Fig. 4. The polygonal grids with $h = \frac{1}{4}, \frac{1}{8}, \frac{1}{16}$.

8.2. Locking-free test

This section is dedicated to the validation of the locking-free property of the CDG scheme (3.3).

Example 8.2. Consider the elasticity problems (1.1) with $\Omega = (0,1)^2$. In this example, we set $\mu = 1$. The exact solution $\boldsymbol{u}$ is

$$\boldsymbol{u} = \begin{pmatrix} \sin(2\pi x)\sin(2\pi y) \\ \cos(2\pi x)\cos(2\pi y) \end{pmatrix} + \frac{1}{\lambda+\mu}\begin{pmatrix} \sin(\pi x)\sin(\pi y) \\ \sin(\pi x)\sin(\pi y) \end{pmatrix},$$

and $\boldsymbol{f}$ is

$$\begin{aligned} \boldsymbol{f} &= -\mu \begin{pmatrix} -8\pi^2 \sin(2\pi x)\sin(2\pi y) \\ -8\pi^2 \cos(2\pi x)\cos(2\pi y) \end{pmatrix} + \frac{2\pi^2\mu}{\lambda+\mu}\begin{pmatrix} \sin(\pi x)\sin(\pi y) \\ \sin(\pi x)\sin(\pi y) \end{pmatrix} \\ &\quad - \begin{pmatrix} \pi^2\cos(\pi x)\cos(\pi y) - \pi^2\sin(\pi x)\sin(\pi y) \\ \pi^2\cos(\pi x)\cos(\pi y) - \pi^2\sin(\pi x)\sin(\pi y) \end{pmatrix}. \end{aligned}$$

In this example, we continue to use triangle meshes, rectangular meshes, deformed rectangular grids, and polygonal meshes for computation correspondingly. In the computation, we set $\lambda = 1$, $\lambda = 10^2$, $\lambda = 10^4$, and $\lambda = 10^6$. The numerical results by the P_2 CDG elements are presented in Tables 5–8.

Table 1
Error and convergence order of displacement $\boldsymbol{u}$ on the uniform triangular grids in Example 8.1.

$1/h$	$\|\|\|\boldsymbol{u}-\boldsymbol{u}_h\|\|\|$	Order	$\|\|\boldsymbol{u}-\boldsymbol{u}_h\|\|$	Order	$\|\|\sigma-\sigma_h\|\|$	Order
By the P_1 CDG element						
8	2.5711E−01	–	3.9205E−02	–	5.2833E−01	–
16	1.1241E−01	1.1936	1.1238E−02	1.8027	2.2769E−01	1.2144
32	5.4191E−02	1.0526	2.9809E−03	1.9145	1.0884E−01	1.0649
64	2.6987E−02	1.0058	7.6563E−04	1.9610	5.4042E−02	1.0100
128	1.3528E−02	0.9964	1.9389E−04	1.9814	2.7065E−02	0.9977
By the P_2 CDG element						
8	2.3980E−02	–	3.3299E−03	–	4.9461E−02	–
16	6.1713E−03	1.9582	4.1413E−04	3.0073	1.2777E−02	1.9528
32	1.5645E−03	1.9798	5.1367E−05	3.0112	3.2419E−03	1.9786
64	3.9376E−04	1.9904	6.3874E−06	3.0076	8.1603E−04	1.9901
128	9.8758E−05	1.9953	7.9606E−07	3.0043	2.0467E−04	1.9953
By the P_3 CDG element						
8	1.5058E−03	–	6.3943E−05	–	3.2397E−03	–
16	1.8382E−04	3.0341	4.0325E−06	3.9871	3.9643E−04	3.0307
32	2.2749E−05	3.0144	2.5629E−07	3.9758	4.9123E−05	3.0126
64	2.8314E−06	3.0062	1.6207E−08	3.9831	6.1180E−06	3.0053
128	3.5324E−07	3.0028	1.0253E−09	3.9825	7.6351E−07	3.0023

Table 2
Error and convergence order of displacement $\boldsymbol{u}$ with the uniform rectangular grids in Example 8.1.

$1/h$	$\|\|\|\boldsymbol{u}-\boldsymbol{u}_h\|\|\|$	Order	$\|\|\boldsymbol{u}-\boldsymbol{u}_h\|\|$	Order	$\|\|\sigma-\sigma_h\|\|$	Order
By the P_1 CDG element						
8	2.5927E−01	–	3.8160E−02	–	5.4332E−01	–
16	7.2981E−02	1.8289	1.0755E−02	1.8271	1.5300E−01	1.8283
32	2.2188E−02	1.7177	2.9833E−03	1.8500	4.6028E−02	1.7329
64	7.0976E−03	1.6444	7.9605E−04	1.9060	1.4550E−02	1.6615
128	2.3536E−03	1.5925	2.0625E−04	1.9485	4.7792E−03	1.6062
By the P_2 CDG element						
8	1.9895E−02	–	5.0457E−03	–	4.0388E−02	–
16	4.2091E−03	2.2408	6.4088E−04	2.9769	8.5211E−03	2.2448
32	9.6374E−04	2.1268	8.0010E−05	3.0018	1.9420E−03	2.1335
64	2.3189E−04	2.0552	9.9720E−06	3.0042	4.6567E−04	2.0602
128	5.7029E−05	2.0237	1.2439E−06	3.0030	1.1430E−04	2.0265
By the P_3 CDG element						
8	2.2612E−03	–	6.7512E−05	–	4.7365E−03	–
16	2.4944E−04	3.1803	2.3942E−06	4.8175	5.1456E−04	3.2024
32	2.9133E−05	3.0980	1.0421E−07	4.5221	5.9440E−05	3.1138
64	3.5180E−06	3.0498	5.4732E−09	4.2509	7.1314E−06	3.0592
128	4.3221E−07	3.0249	3.1888E−10	4.1013	8.7309E−07	3.0300

Based on the results presented in Tables 5–8, it is evident that the error and convergence order remain unaffected by the parameter λ. This observation indicates that the CDG numerical scheme is devoid of the locking phenomenon, corroborating the findings of previous theoretical analysis.

8.3. Cook's membrane

In the following example, we consider the following linear elasticity problem:

$$-\nabla\cdot\sigma(\boldsymbol{u})=\boldsymbol{f},\quad \text{in } \Omega, \tag{8.1a}$$

$$\boldsymbol{u}=\boldsymbol{g},\quad \text{on } \Gamma_D, \tag{8.1b}$$

$$\sigma\boldsymbol{n}=\boldsymbol{t},\quad \text{on } \Gamma_N, \tag{8.1c}$$

where Γ_D and Γ_N are nonempty sets, satisfies $\Gamma_D\cup\Gamma_N=\partial\Omega$, $\Gamma_D\cap\Gamma_N=\emptyset$, and $\boldsymbol{n}$ is unit outward normal vector on $\partial\Omega$.

We use the CDG method to solve the Cook's membrane problem as shown in Fig. 5. Here $\partial\Omega=\Gamma_1\cup\Gamma_2\cup\Gamma_3\cup\Gamma_4$. In this example, the body force is $\boldsymbol{f}=(0,0)^T$, and the boundary conditions are $\boldsymbol{u}|_{\Gamma_1}=(0,0)^T$, $\sigma\boldsymbol{n}|_{\Gamma_2}=(0,0)^T$, $\sigma\boldsymbol{n}|_{\Gamma_3}=(0,\frac{1}{16})^T$, and $\sigma\boldsymbol{n}|_{\Gamma_4}=(0,0)^T$.

In this example, we consider two cases [38,48]:

(a) Compressible case: a material with Young's modulus $E=1$ and Poisson's ratio $\nu=\frac{1}{3}$.

(b) Nearly incompressible case: a material with Young's modulus $E=1.12499998125$ and Poisson's ratio $\nu=0.499999975$.

Table 3
Error and convergence order of displacement $\boldsymbol{u}$ with the deformed rectangular grids in Example 8.1.

$1/h$	$\|\|\|\boldsymbol{u}-\boldsymbol{u}_h\|\|\|$	Order	$\|\boldsymbol{u}-\boldsymbol{u}_h\|$	Order	$\|\sigma-\sigma_h\|$	Order
By the P_1 CDG element						
8	4.2876E−01	–	5.3211E−02	–	9.2688E−01	–
16	1.3803E−01	1.6705	1.7179E−02	1.6664	3.0350E−01	1.6455
32	3.8641E−02	1.8467	5.0223E−03	1.7837	8.4441E−02	1.8556
64	1.0585E−02	1.8707	1.3472E−03	1.9010	2.2830E−02	1.8895
128	2.9889E−03	1.8249	3.4761E−04	1.9550	6.3496E−03	1.8468
By the P_2 CDG element						
8	4.0905E−02	–	7.2882E−03	–	8.3401E−02	–
16	8.8334E−03	2.2590	9.8180E−04	2.9546	1.7880E−02	2.2698
32	1.9891E−03	2.1624	1.2387E−04	3.0027	4.0089E−03	2.1687
64	4.7702E−04	2.0628	1.5440E−05	3.0081	9.5802E−04	2.0678
128	1.1765E−04	2.0202	1.9233E−06	3.0060	2.3580E−04	2.0231
By the P_3 CDG element						
8	4.2611E−03	–	1.8276E−04	–	8.9240E−03	–
16	5.1646E−04	3.1103	1.1709E−05	4.0500	1.0715E−03	3.1242
32	6.1701E−05	3.0818	7.3626E−07	4.0127	1.2694E−04	3.0940
64	7.5487E−06	3.0350	4.6112E−08	4.0024	1.5470E−05	3.0407
128	9.3590E−07	3.0128	2.8853E−09	3.9997	1.9151E−06	3.0150

Table 4
Error and convergence order of displacement $\boldsymbol{u}$ with the polygonal grids in Example 8.1.

$1/h$	$\|\|\|\boldsymbol{u}-\boldsymbol{u}_h\|\|\|$	Order	$\|\boldsymbol{u}-\boldsymbol{u}_h\|$	Order	$\|\sigma-\sigma_h\|$	Order
By the P_1 CDG element						
8	3.7824E−01	–	3.8195E−02	–	7.9946E−01	–
16	1.2203E−01	1.6321	1.1875E−02	1.6855	2.5778E−01	1.6329
32	3.9148E−02	1.6402	3.2352E−03	1.8760	8.2272E−02	1.6477
64	1.2896E−02	1.6020	8.3981E−04	1.9457	2.6951E−02	1.6101
128	4.3649E−03	1.5629	2.1366E−04	1.9747	9.0814E−03	1.5693
By the P_2 CDG element						
8	5.2092E−02	–	1.3895E−03	–	1.0446E−01	–
16	1.3142E−02	1.9869	1.6445E−04	3.0789	2.6305E−02	1.9895
32	3.2785E−03	2.0031	1.9746E−05	3.0581	6.5590E−03	2.0038
64	8.1826E−04	2.0024	2.4141E−06	3.0320	1.6367E−03	2.0027
128	2.0439E−04	2.0012	2.9843E−07	3.0160	4.0880E−04	2.0013
By the P_3 CDG element						
8	2.3563E−03	–	2.5729E−05	–	4.8698E−03	–
16	2.4288E−04	3.2782	1.5784E−06	4.0269	5.0988E−04	3.2556
32	2.6572E−05	3.1923	9.8161E−08	4.0072	5.6579E−05	3.1718
64	3.0917E−06	3.1034	6.1325E−09	4.0006	6.6451E−06	3.0899
128	3.7305E−07	3.0510	3.9631E−10	3.9518	8.0600E−07	3.0434

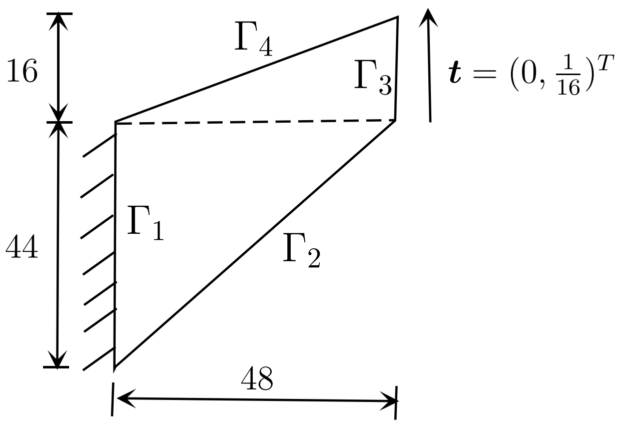

Fig. 5. The illustration for Cook's membrane.

Table 5
Error and convergence order of displacement $\boldsymbol{u}$ on the uniform triangular grids in Example 8.2.

$1/h$	$\|\|\|\boldsymbol{u}-\boldsymbol{u}_h\|\|\|$	Order	$\|\boldsymbol{u}-\boldsymbol{u}_h\|$	Order	$\|\sigma-\sigma_h\|$	Order
By the P_2 CDG element with $\lambda=1$						
8	2.0339E−01	–	1.1921E−02	–	4.7872E−01	–
16	5.1567E−02	1.9797	1.5289E−03	2.9630	1.1463E−01	2.0622
32	1.3000E−02	1.9879	1.8970E−04	3.0106	2.7879E−02	2.0397
64	3.2645E−03	1.9937	2.3509E−05	3.0127	6.8655E−03	2.0218
128	8.1800E−04	1.9966	2.9200E−06	3.0090	1.7029E−03	2.0113
By the P_2 CDG element with $\lambda=10^2$						
8	2.3004E−01	–	1.9420E−02	–	7.4057E−01	–
16	5.3639E−02	2.1005	2.4026E−03	3.0148	1.5938E−01	2.2161
32	1.3181E−02	2.0248	3.0018E−04	3.0007	3.7484E−02	2.0881
64	3.2844E−03	2.0049	3.7582E−05	2.9979	9.1292E−03	2.0377
128	8.2100E−04	2.0001	4.7000E−06	2.9992	2.2554E−03	2.0171
By the P_2 CDG element with $\lambda=10^4$						
8	2.3214E−01	–	1.9656E−02	–	7.5473E−01	–
16	5.3912E−02	2.1063	2.4429E−03	3.0083	1.6201E−01	2.2199
32	1.3232E−02	2.0266	3.0579E−04	2.9980	3.8057E−02	2.0898
64	3.2959E−03	2.0053	3.8320E−05	2.9964	9.2651E−03	2.0383
128	8.2365E−04	2.0006	4.7986E−06	2.9974	2.2887E−03	2.0173
By the P_2 CDG element with $\lambda=10^6$						
8	2.3216E−01	–	1.9659E−02	–	7.5488E−01	–
16	5.3915E−02	2.1064	2.4433E−03	3.0083	1.6204E−01	2.2199
32	1.3233E−02	2.0266	3.0585E−04	2.9980	3.8063E−02	2.0898
64	3.2960E−03	2.0053	3.8329E−05	2.9963	9.2665E−03	2.0383
128	8.2368E−04	2.0006	4.8011E−06	2.9970	2.2891E−03	2.0173

Table 6
Error and convergence order of displacement $\boldsymbol{u}$ on the uniform rectangular grids in Example 8.2.

$1/h$	$\|\|\|\boldsymbol{u}-\boldsymbol{u}_h\|\|\|$	Order	$\|\boldsymbol{u}-\boldsymbol{u}_h\|$	Order	$\|\sigma-\sigma_h\|$	Order
By the P_2 CDG element with $\lambda=1$						
8	2.2394E−01	–	1.7490E−02	–	6.0087E−01	–
16	4.2217E−02	2.4072	2.2402E−03	2.9648	1.1317E−01	2.4085
32	9.1239E−03	2.2101	2.7599E−04	3.0209	2.2707E−02	2.3173
64	2.1710E−03	2.0713	3.4022E−05	3.0201	4.9607E−03	2.1945
128	5.3517E−04	2.0203	4.2165E−06	3.0123	1.1515E−03	2.1070
By the P_2 CDG element with $\lambda=10^2$						
8	2.3767E−01	–	1.9177E−02	–	7.5033E−01	–
16	4.2907E−02	2.4696	2.6802E−03	2.8389	1.2264E−01	2.6130
32	9.0779E−03	2.2408	3.4579E−04	2.9544	2.3356E−02	2.3926
64	2.1467E−03	2.0803	4.3594E−05	2.9877	4.9915E−03	2.2262
128	5.2865E−04	2.0217	5.4618E−06	2.9967	1.1476E−03	2.1209
By the P_2 CDG element with $\lambda=10^4$						
8	2.3908E−01	–	1.9186E−02	–	7.6535E−01	–
16	4.2990E−02	2.4754	2.6947E−03	2.8319	1.2350E−01	2.6316
32	9.0816E−03	2.2430	3.4878E−04	2.9498	2.3417E−02	2.3989
64	2.1465E−03	2.0809	4.4038E−05	2.9855	4.9967E−03	2.2285
128	5.2857E−04	2.0219	5.5213E−06	2.9957	1.1480E−03	2.1218
By the P_2 CDG element with $\lambda=10^6$						
8	2.3910E−01	–	1.9186E−02	–	7.6551E−01	–
16	4.2991E−02	2.4755	2.6949E−03	2.8318	1.2351E−01	2.6318
32	9.0816E−03	2.2430	3.4881E−04	2.9497	2.3417E−02	2.3989
64	2.1465E−03	2.0809	4.4041E−05	2.9855	4.9967E−03	2.2285
128	5.2857E−04	2.0219	5.4953E−06	3.0026	1.1480E−03	2.1218

According to [48], the reference values are 21.520 (compressible case) and 16.442 (nearly incompressible case) on $u_2(48,52)$. We use the CDG method, the stabilizer-free weak Galerkin (SFWG) method, and the simplified weak Galerkin (SWG) method [38] to solve the Cook's membrane problem. The numerical results are shown in Figs. 6–9. As we can see, the CDG method quickly converges to the reference value at $u_2(48,52)$. When targeting the same approximate values $u_2(48,52)$, the CDG method uses significantly fewer degrees of freedom than the SFWG and SWG methods. This demonstrates that the CDG method outperforms the SFWG and SWG methods.

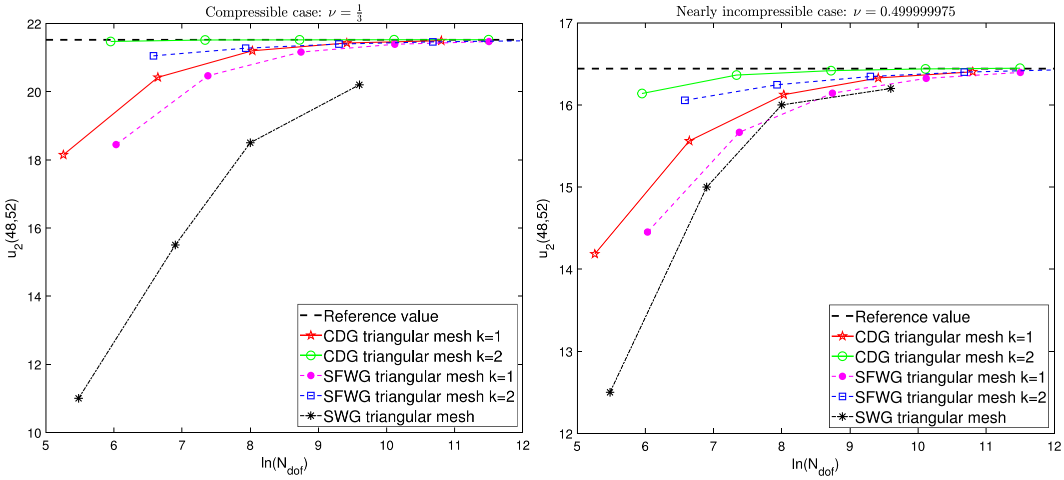

Fig. 6. Convergence performance of the Cook's membrane test on the triangular meshes.

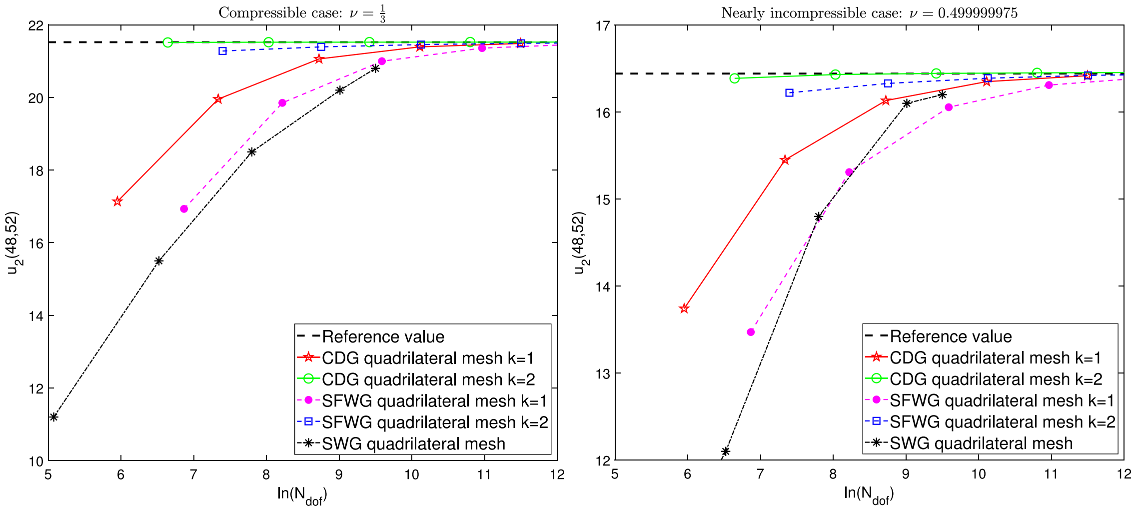

Fig. 7. Convergence performance of the Cook's membrane test on the quadrilateral meshes.

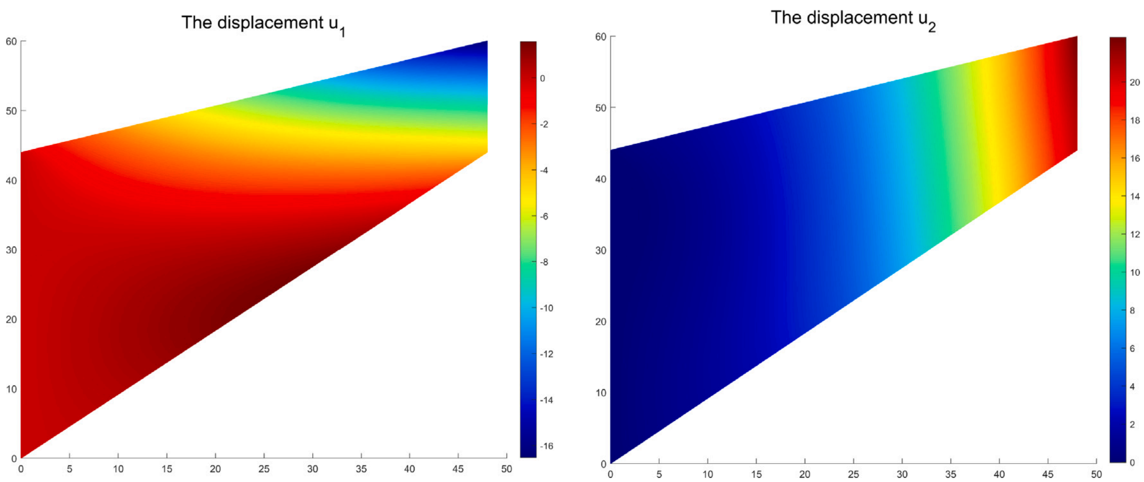

Fig. 8. The displacement of the Cook's membrane test using the P_1 CDG element on the triangular mesh with $n = 32$ when $E = 1$ and $\nu = \frac{1}{3}$.

Table 7
Error and convergence order of displacement $\boldsymbol{u}$ on the deformed rectangular grids in Example 8.2.

$1/h$	$\|\|\|\boldsymbol{u}-\boldsymbol{u}_h\|\|\|$	Order	$\|\boldsymbol{u}-\boldsymbol{u}_h\|$	Order	$\|\sigma-\sigma_h\|$	Order
By the P_2 CDG element with $\lambda=1$						
8	4.7909E−01	–	3.2511E−02	–	1.2277E+00	–
16	1.0239E−01	2.2743	4.4132E−03	2.9433	3.2574E−01	1.9142
32	2.1755E−02	2.2467	5.4802E−04	3.0257	6.1226E−02	2.4115
64	5.0483E−03	2.1103	6.7811E−05	3.0187	1.3829E−02	2.1465
128	1.2339E−03	2.0332	8.4079E−06	3.0127	3.3365E−03	2.0513
By the P_2 CDG element with $\lambda=10^2$						
8	5.0531E−01	–	3.8612E−02	–	1.3890E+00	–
16	1.0550E−01	2.3088	5.1543E−03	2.9680	3.4938E−01	1.9912
32	2.1957E−02	2.2766	6.5726E−04	2.9872	9.7724E−02	1.8380
64	5.0501E−03	2.1232	8.2398E−05	2.9998	2.7356E−02	1.8368
128	1.2311E−03	2.0370	1.0288E−05	3.0027	7.3156E−03	1.9028
By the P_2 CDG element with $\lambda=10^4$						
8	5.0688E−01	–	3.8089E−02	–	1.4153E+00	–
16	1.0573E−01	2.3102	5.1782E−03	2.9411	3.5212E−01	2.0070
32	2.1971E−02	2.2788	6.6194E−04	2.9836	9.7633E−02	1.8506
64	5.0510E−03	2.1238	8.3078E−05	2.9982	2.7251E−02	1.8410
128	1.2312E−03	2.0372	1.0379E−05	3.0019	7.2799E−03	1.9043
By the P_2 CDG element with $\lambda=10^6$						
8	5.0690E−01	–	3.8087E−02	–	1.4156E+00	–
16	1.0573E−01	2.3102	5.1785E−03	2.9409	3.5215E−01	2.0072
32	2.1972E−02	2.2789	6.6198E−04	2.9836	9.7633E−02	1.8508
64	5.0510E−03	2.1239	8.3085E−05	2.9981	2.7250E−02	1.8411
128	1.2312E−03	2.0372	1.0378E−05	3.0020	7.2796E−03	1.9044

Table 8
Error and convergence order of displacement $\boldsymbol{u}$ on the polygonal grids in Example 8.2.

$1/h$	$\|\|\|\boldsymbol{u}-\boldsymbol{u}_h\|\|\|$	Order	$\|\boldsymbol{u}-\boldsymbol{u}_h\|$	Order	$\|\sigma-\sigma_h\|$	Order
By the P_2 CDG element with $\lambda=1$						
8	2.4668E−01	–	1.2861E−02	–	5.4213E−01	–
16	5.4783E−02	2.1708	1.2198E−03	3.3982	1.2478E−01	2.1192
32	1.2630E−02	2.1169	1.1246E−04	3.4392	2.8957E−02	2.1074
64	3.0156E−03	2.0663	1.1470E−05	3.2936	6.8878E−03	2.0718
128	7.3600E−04	2.0347	1.2800E−06	3.1636	1.6729E−03	2.0417
By the P_2 CDG element with $\lambda=10^2$						
8	2.3896E−01	–	1.1992E−02	–	6.0152E−01	–
16	5.3122E−02	2.1694	1.1486E−03	3.3841	1.3072E−01	2.2021
32	1.2307E−02	2.1098	1.0939E−04	3.3923	2.9524E−02	2.1465
64	2.9489E−03	2.0612	1.1604E−05	3.2369	6.9254E−03	2.0919
128	7.2100E−04	2.0321	1.3400E−06	3.1143	1.6692E−03	2.0527
By the P_2 CDG element with $\lambda=10^4$						
8	2.3921E−01	–	1.1853E−02	–	6.1273E−01	–
16	5.3121E−02	2.1709	1.1372E−03	3.3817	1.3161E−01	2.2190
32	1.2306E−02	2.1099	1.0851E−04	3.3895	2.9627E−02	2.1513
64	2.9487E−03	2.0612	1.1539E−05	3.2332	6.9393E−03	2.0940
128	7.2081E−04	2.0324	1.3304E−06	3.1166	1.6713E−03	2.0539
By the P_2 CDG element with $\lambda=10^6$						
8	2.3921E−01	–	1.1851E−02	–	6.1292E−01	–
16	5.3121E−02	2.1709	1.1370E−03	3.3817	1.3162E−01	2.2193
32	1.2306E−02	2.1099	1.0850E−04	3.3894	2.9628E−02	2.1514
64	2.9487E−03	2.0612	1.1537E−05	3.2334	6.9395E−03	2.0941
128	7.2081E−04	2.0324	1.3234E−06	3.1239	1.6713E−03	2.0539

9. Conclusions

In this paper, we present the definitions and properties for the discrete weak gradient and weak divergence of vector-valued functions. Additionally, we propose a conforming discontinuous Galerkin (CDG) method for linear elasticity problems grounded in the primal formulation. Then, we find the equivalence of the CDG schemes between the primal formulation and the mixed formulation and prove the locking-free characteristic of the CDG scheme for the primal one by establishing optimal order error

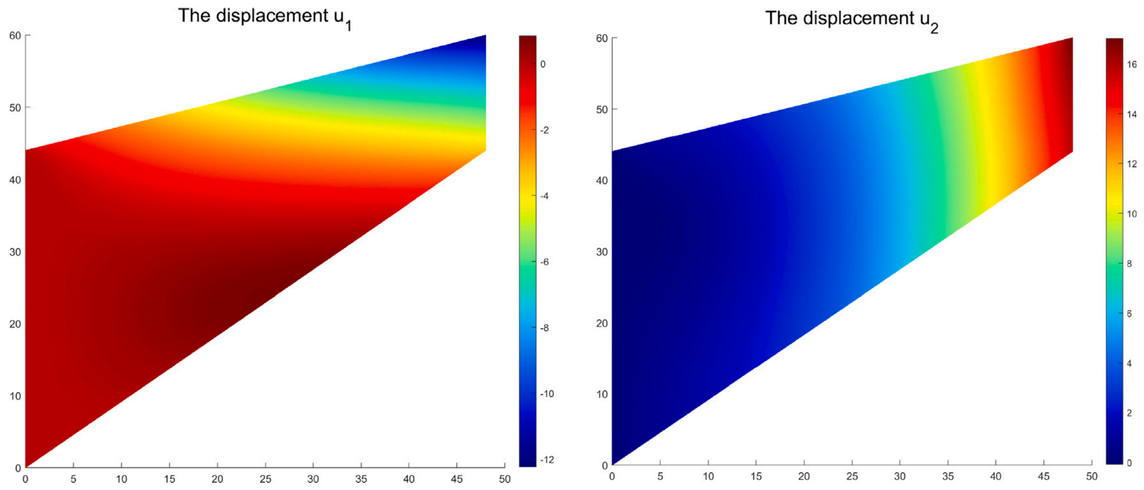

Fig. 9. The displacement of the Cook's membrane test using the P_1 CDG element on the triangular mesh with $n = 32$ when $E = 1.12499998125$ and $\nu = 0.499999975$.

estimates in both H^1-norm and L^2-norm. Numerical results are presented to validate the effectiveness and locking-free characteristics of the proposed methods for the linear elasticity problems.

Acknowledgments

The research was supported by the National Key R&D Program of China (grant No. 2020YFA0713602, 2023YFA1008803), the National Natural Science Foundation of China (grant No. 11971198, 12001230, 12001232, 22341302), and the Key Laboratory of Symbolic Computation and Knowledge Engineering of Ministry of Education of China housed at Jilin University.

Appendix. Some inequality estimates

Lemma A.1. *For any $\boldsymbol{w} \in [H^{k+1}(\Omega)]^d$, $\rho \in H^k(\Omega)$, and $\boldsymbol{v} \in V_h$, we have*

$$|l(\boldsymbol{w}, \boldsymbol{v})| \leq Ch^k \|\boldsymbol{w}\|_{k+1} \, ||| \boldsymbol{v} |||, \tag{A.1a}$$

$$|\theta(\rho, \boldsymbol{v})| \leq Ch^k \|\rho\|_k \, ||| \boldsymbol{v} ||| \,. \tag{A.1b}$$

Proof. By using the Cauchy–Schwarz inequality, trace inequality [41], projection inequality [42], and Lemma 4.1, we get

$$\begin{aligned}
|l(\boldsymbol{w}, \boldsymbol{v})| &= \left| \sum_{T \in \mathcal{T}_h} \langle \boldsymbol{v} - \{\boldsymbol{v}\}, 2\mu(\varepsilon(\boldsymbol{u}) - \boldsymbol{Q}_h \varepsilon(\boldsymbol{u})) \cdot \boldsymbol{n} \rangle \right| \\
&\leq C \left(\sum_{T \in \mathcal{T}_h} h_T^{-1} \|\boldsymbol{v} - \{\boldsymbol{v}\}\|_{\partial T}^2 \right)^{1/2} \left(\sum_{T \in \mathcal{T}_h} h_T \|\varepsilon(\boldsymbol{w}) - \boldsymbol{Q}_h \varepsilon(\boldsymbol{w})\|_{\partial T}^2 \right)^{1/2} \\
&\leq Ch^k \|\boldsymbol{w}\|_{k+1} \, ||| \boldsymbol{v} ||| \,.
\end{aligned}$$

Similarly, from the Cauchy–Schwarz inequality, trace inequality, projection inequality, and Lemma 4.1, we obtain

$$\begin{aligned}
|\theta(\rho, \boldsymbol{v})| &= \left| \sum_{T \in \mathcal{T}_h} \langle \boldsymbol{v} - \{\boldsymbol{v}\}, (\rho - \mathbb{Q}_h \rho) \boldsymbol{n} \rangle_{\partial T} \right| \\
&\leq C \left(\sum_{T \in \mathcal{T}_h} h_T^{-1} \|\boldsymbol{v} - \{\boldsymbol{v}\}\|_{\partial T}^2 \right)^{1/2} \left(\sum_{T \in \mathcal{T}_h} h_T \|\rho - \mathbb{Q}_h \rho\|_{\partial T}^2 \right)^{1/2} \\
&\leq C \, ||| \boldsymbol{v} ||| \left(\sum_{T \in \mathcal{T}_h} \|\rho - \mathbb{Q}_h \rho\|_T^2 \right)^{1/2} \\
&\leq Ch^k \|\rho\|_k \, ||| \boldsymbol{v} ||| \,. \quad \square
\end{aligned}$$

Lemma A.2. *For any $\boldsymbol{w} \in [H^{k+1}(\Omega)]^d$, there holds*

$$|||\boldsymbol{w} - Q_h\boldsymbol{w}||| \le Ch^k \|\boldsymbol{w}\|_{k+1}. \tag{A.2}$$

Proof. For any $\tau \in [P_j(T)]^{d\times d}$, according to the definition of discrete weak strain, integration by parts, trace inequality, inverse inequality [42], and projection inequality, we derive

$$\begin{aligned}
(\varepsilon_w(\boldsymbol{w} - Q_h\boldsymbol{w}), \tau)_T &= \frac{1}{2}(\nabla_w(\boldsymbol{w} - Q_h\boldsymbol{w}), \tau + \tau^T)_T \\
&= -\frac{1}{2}(\boldsymbol{w} - Q_h\boldsymbol{w}, \nabla\cdot(\tau+\tau^T))_T + \frac{1}{2}\langle\{\boldsymbol{w} - Q_h\boldsymbol{w}\}, (\tau+\tau^T)\cdot\boldsymbol{n}\rangle_{\partial T} \\
&= \frac{1}{2}(\nabla(\boldsymbol{w} - Q_h\boldsymbol{w}), \tau+\tau^T) + \frac{1}{2}\langle\{\boldsymbol{w} - Q_h\boldsymbol{w}\} - (\boldsymbol{w} - Q_h\boldsymbol{w}), (\tau+\tau^T)\cdot\boldsymbol{n}\rangle_{\partial T} \\
&\le C\|\nabla(\boldsymbol{w} - Q_h\boldsymbol{w})\|_T\|\tau+\tau^T\|_T + Ch^{-1/2}\|[\boldsymbol{w} - Q_h\boldsymbol{w}]\|_{\partial T}\,\|\tau+\tau^T\|_T \\
&\le C\left(\|\nabla(\boldsymbol{w} - Q_h\boldsymbol{w})\|_T + h^{-1/2}\|[\boldsymbol{w} - Q_h\boldsymbol{w}]\|_{\partial T}\right)\|\tau\|_T \\
&\le Ch^k\|\boldsymbol{w}\|_{k+1,T}\|\tau\|_T.
\end{aligned}$$

Letting $\tau = \varepsilon_w(\boldsymbol{w} - Q_h\boldsymbol{w})$, the desired inequality is obtained. □

Lemma A.3. *For any $\boldsymbol{w} \in [H^{k+1}(\Omega)]^d$ and $q \in W_h$, we have*

$$(\nabla\cdot\boldsymbol{w}, q) = (\nabla_w\cdot Q_h\boldsymbol{w}, q) + \chi(\boldsymbol{w}, q), \tag{A.3}$$

and

$$|\chi(\boldsymbol{w}, q)| \le Ch^k\|\boldsymbol{w}\|_{k+1}\|q\|, \tag{A.4}$$

where

$$\chi(\boldsymbol{w}, q) = \sum_{T\in\mathcal{T}_h}\langle\{\boldsymbol{w} - Q_h\boldsymbol{w}\}\cdot\boldsymbol{n}, q\rangle_{\partial T}.$$

Proof. By using integration by parts and the definition of discrete weak divergence, it follows that

$$\begin{aligned}
(\nabla\cdot\boldsymbol{w}, q) &= -\sum_{T\in\mathcal{T}_h}(\boldsymbol{w}, \nabla q)_T + \sum_{T\in\mathcal{T}_h}\langle\boldsymbol{w}\cdot\boldsymbol{n}, q\rangle_{\partial T} \\
&= -\sum_{T\in\mathcal{T}_h}(Q_h\boldsymbol{w}, \nabla q)_T + \sum_{T\in\mathcal{T}_h}\langle\boldsymbol{w}\cdot\boldsymbol{n}, q\rangle_{\partial T} \\
&= (\nabla_w\cdot Q_h\boldsymbol{w}, q) + \sum_{T\in\mathcal{T}_h}\langle\{\boldsymbol{w} - Q_h\boldsymbol{w}\}\cdot\boldsymbol{n}, q\rangle_{\partial T} \\
&= (\nabla_w\cdot Q_h\boldsymbol{w}, q) + \chi(\boldsymbol{w}, q).
\end{aligned}$$

From the Cauchy–Schwarz inequality, trace inequality, and projection inequality, we get

$$\begin{aligned}
|\chi(\boldsymbol{w}, q)| &= \left|\sum_{T\in\mathcal{T}_h}\langle\{\boldsymbol{w} - Q_h\boldsymbol{w}\}\cdot\boldsymbol{n}, q\rangle_{\partial T}\right| \\
&\le C\left(\sum_{T\in\mathcal{T}_h} h_T^{-1}\|\boldsymbol{w} - Q_h\boldsymbol{w}\|_{\partial T}^2\right)^{1/2}\left(\sum_{T\in\mathcal{T}_h} h_T\|q\|_{\partial T}^2\right)^{1/2} \\
&\le Ch^k\|\boldsymbol{w}\|_{k+1}\|q\|. \quad \square
\end{aligned}$$

Lemma A.4. *For I_i defined in (7.8), we have the following estimates:*

$$|I_1| \le Ch^{k+1}\|\boldsymbol{u}\|_{k+1}\|\boldsymbol{\psi}\|_2, \tag{A.5a}$$

$$|I_2| \le Ch^{k+1}(\|\boldsymbol{u}\|_{k+1} + \|p\|_k)\|\boldsymbol{\psi}\|_2, \tag{A.5b}$$

$$|I_3| \le Ch^{k+1}\|\boldsymbol{u}\|_{k+1}\|\boldsymbol{\psi}\|_2, \tag{A.5c}$$

$$|I_4| \le Ch^{k+1}\|p\|_k\|\boldsymbol{\psi}\|_2, \tag{A.5d}$$

$$|I_5| \le Ch^{k+1}(\|\boldsymbol{u}\|_{k+1} + \|p\|_k)\|\boldsymbol{\psi}\|_2, \tag{A.5e}$$

$$|I_6| \le Ch^{k+1}(\|\boldsymbol{u}\|_{k+1} + \|p\|_k)\|\phi\|_1, \tag{A.5f}$$

$$|I_7| \le Ch^{k+1}\|\boldsymbol{u}\|_{k+1}\|\phi\|_1, \tag{A.5g}$$

$$|I_8| \le Ch^{k+1}(\|\boldsymbol{u}\|_{k+1} + \|p\|_k)\|\boldsymbol{\psi}\|_2. \tag{A.5h}$$

Proof. For $|I_1|$, according to (5.3) and the triangle inequality, we obtain

$$
\begin{aligned}
|I_1| &= \left|\sum_{T\in\mathcal{T}_h} 2\mu(\varepsilon_w(\boldsymbol{u}-Q_h\boldsymbol{u}),\varepsilon_w(\boldsymbol{\psi}))_T\right| \\
&= \left|\sum_{T\in\mathcal{T}_h} 2\mu(\varepsilon_w(\boldsymbol{u}-Q_h\boldsymbol{u}),\boldsymbol{Q}_h\varepsilon(\boldsymbol{\psi}))_T\right| \\
&= \left|\sum_{T\in\mathcal{T}_h} 2\mu(\varepsilon_w(\boldsymbol{u}-Q_h\boldsymbol{u}),\boldsymbol{Q}_h\varepsilon(\boldsymbol{\psi})-\varepsilon(\boldsymbol{\psi})+\varepsilon(\boldsymbol{\psi}))_T\right| \\
&\le \left|\sum_{T\in\mathcal{T}_h} 2\mu(\varepsilon_w(\boldsymbol{u}-Q_h\boldsymbol{u}),\boldsymbol{Q}_h\varepsilon(\boldsymbol{\psi})-\varepsilon(\boldsymbol{\psi}))_T\right| \\
&\quad + \left|\sum_{T\in\mathcal{T}_h} 2\mu(\varepsilon_w(\boldsymbol{u}-Q_h\boldsymbol{u}),\varepsilon(\boldsymbol{\psi}))_T\right| \\
&:= J_1 + J_2.
\end{aligned} \tag{A.6}
$$

By using the projection inequality, it follows that

$$
\begin{aligned}
J_1 &\le C\left(\sum_{T\in\mathcal{T}_h}\|\varepsilon_w(\boldsymbol{u}-Q_h\boldsymbol{u})\|_T^2\right)^{1/2}\left(\sum_{T\in\mathcal{T}_h}\|\varepsilon(\boldsymbol{\psi})-\boldsymbol{Q}_h\varepsilon(\boldsymbol{\psi})\|_T^2\right)^{1/2} \\
&\le Ch^{k+1}\|\boldsymbol{u}\|_{k+1}\|\boldsymbol{\psi}\|_2,
\end{aligned} \tag{A.7}
$$

and

$$
\begin{aligned}
J_2 &= \left|-\sum_{T\in\mathcal{T}_h} 2\mu(Q_h\boldsymbol{u}-\boldsymbol{u},\nabla\cdot\varepsilon(\boldsymbol{\psi}))_T + \sum_{T\in\mathcal{T}_h} 2\mu\langle\{Q_h\boldsymbol{u}-\boldsymbol{u}\},\varepsilon(\boldsymbol{\psi})\cdot\boldsymbol{n}\rangle_{\partial T}\right| \\
&= \left|-\sum_{T\in\mathcal{T}_h} 2\mu(Q_h\boldsymbol{u}-\boldsymbol{u},\nabla\cdot\varepsilon(\boldsymbol{\psi}))_T\right| \\
&\le Ch^{k+1}\|\boldsymbol{u}\|_{k+1}\|\boldsymbol{\psi}\|_2,
\end{aligned} \tag{A.8}
$$

which yields

$$
|I_1| \le Ch^{k+1}\|\boldsymbol{u}\|_{k+1}\|\boldsymbol{\psi}\|_2. \tag{A.9}
$$

For $|I_2|$, by Lemma 5.4 and Theorem 6.1, we have

$$
\begin{aligned}
|I_2| &\le \left|\sum_{T\in\mathcal{T}_h} 2\mu(\varepsilon_w(\boldsymbol{e}_h),\varepsilon_w(\boldsymbol{\psi}-Q_h\boldsymbol{\psi}))_T\right| \\
&\le C\,|||\,\boldsymbol{e}_h\,|||\;|||\boldsymbol{\psi}-Q_h\boldsymbol{\psi}||| \\
&\le Ch^{k+1}(\|\boldsymbol{u}\|_{k+1}+\|p\|_k)\|\boldsymbol{\psi}\|_2.
\end{aligned} \tag{A.10}
$$

For $|I_3|$, from the Cauchy–Schwarz inequality, trace inequality, and projection inequality, we get

$$
\begin{aligned}
|I_3| &= \left|\sum_{T\in\mathcal{T}_h}\langle Q_h\boldsymbol{\psi}-\{Q_h\boldsymbol{\psi}\},2\mu(\varepsilon(\boldsymbol{u})-Q_h\varepsilon(\boldsymbol{u}))\cdot\boldsymbol{n}\rangle_{\partial T}\right| \\
&= \left|\sum_{T\in\mathcal{T}_h}\langle Q_h\boldsymbol{\psi}-\boldsymbol{\psi}+\{\boldsymbol{\psi}-Q_h\boldsymbol{\psi}\},2\mu(\varepsilon(\boldsymbol{u})-Q_h\varepsilon(\boldsymbol{u}))\cdot\boldsymbol{n}\rangle_{\partial T}\right| \\
&\le C\left(\sum_{T\in\mathcal{T}_h} h_T^{-1}\|\boldsymbol{\psi}-Q_h\boldsymbol{\psi}\|_T^2\right)^{1/2}\left(\sum_{T\in\mathcal{T}_h} h_T\|\varepsilon(\boldsymbol{u})-Q_h\varepsilon(\boldsymbol{u})\|_T^2\right)^{1/2} \\
&\le Ch^{k+1}\|\boldsymbol{u}\|_{k+1}\|\boldsymbol{\psi}\|_2.
\end{aligned} \tag{A.11}
$$

Similarly, for $|I_4|$, it is simple to get that

$$\begin{aligned}|I_4| &= \left|\sum_{T\in\mathcal{T}_h}\langle Q_h\boldsymbol{\psi}-\{Q_h\boldsymbol{\psi}\},(p-\mathbb{Q}_hp)\boldsymbol{n}\rangle_{\partial T}\right|\\ &= \left|\sum_{T\in\mathcal{T}_h}\langle Q_h\boldsymbol{\psi}-\boldsymbol{\psi}+\{\boldsymbol{\psi}-Q_h\boldsymbol{\psi}\},(p-\mathbb{Q}_hp)\boldsymbol{n}\rangle_{\partial T}\right|\\ &\le C\left(\sum_{T\in\mathcal{T}_h}h_T^{-1}\|\boldsymbol{\psi}-Q_h\boldsymbol{\psi}\|_T^2\right)^{1/2}\left(\sum_{T\in\mathcal{T}_h}h_T\|p-\mathbb{Q}_hp\|_T^2\right)^{1/2}\\ &\le Ch^{k+1}\|p\|_k\|\boldsymbol{\psi}\|_2.\end{aligned} \tag{A.12}$$

For $|I_5|,|I_6|$, by using Lemmas 5.3, 5.4, and Theorem 6.1, we have

$$\begin{aligned}|I_5| &\le Ch\|\boldsymbol{\psi}\|_2 ||| \boldsymbol{\rho}_h|||\\ &\le Ch\|\boldsymbol{\psi}\|_2(|||\boldsymbol{e}_h ||| + ||| \boldsymbol{u}-Q_h\boldsymbol{u}|||)\\ &\le Ch^{k+1}(\|\boldsymbol{u}\|_{k+1}+\|p\|_k)\|\boldsymbol{\psi}\|_2,\end{aligned} \tag{A.13}$$

and

$$\begin{aligned}|I_6| &\le Ch\|\phi\|_1 ||| \boldsymbol{\rho}_h|||\\ &\le Ch^{k+1}(\|\boldsymbol{u}\|_{k+1}+\|p\|_k)\|\phi\|_1.\end{aligned} \tag{A.14}$$

For $|I_7|$, it follows from the fact that $\chi(\boldsymbol{u},\phi)=0$, Cauchy–Schwarz inequality, trace inequality, and projection inequality that

$$\begin{aligned}|I_7| &= |\chi(\boldsymbol{u},\mathbb{Q}_h\phi-\phi)+\chi(\boldsymbol{u},\phi)|\\ &= |\chi(\boldsymbol{u},\mathbb{Q}_h\phi-\phi)|\\ &\le Ch^k\|\boldsymbol{u}\|_{k+1}\|\mathbb{Q}_h\phi-\phi\|\\ &\le Ch^{k+1}\|\boldsymbol{u}\|_{k+1}\|\phi\|_1.\end{aligned} \tag{A.15}$$

For $|I_8|$, according to Lemma 5.5 and Theorem 6.1, we derive

$$\begin{aligned}|I_8| &\le Ch\|\boldsymbol{\psi}\|_2\|\xi_h\|\\ &\le Ch^{k+1}(\|\boldsymbol{u}\|_{k+1}+\|p\|_k)\|\boldsymbol{\psi}\|_2.\end{aligned} \tag{A.16}$$

The proof is completed. □

Data availability

Data will be made available on request.

References

[1] A.P. Boresi, K. Chong, J.D. Lee, Elasticity in Engineering Mechanics, John Wiley & Sons, 2010.
[2] W.J. Layton, F. Schieweck, I. Yotov, Coupling fluid flow with porous media flow, SIAM J. Numer. Anal. 40 (2002) 2195–2218.
[3] H. Rui, M. Sun, A locking-free finite difference method on staggered grids for linear elasticity problems, Comput. Math. Appl. 76 (2018) 1301–1320.
[4] Z. Zhao, H. Dong, W. Ying, Kernel free boundary integral method for 3D incompressible flow and linear elasticity equations on irregular domains, Comput. Methods Appl. Mech. Engrg. 414 (2023) 23, Paper (116163).
[5] I. Babuška, M. Suri, On locking and robustness in the finite element method, SIAM J. Numer. Anal. 29 (1992) 1261–1293.
[6] C. Carstensen, H. Rabus, The adaptive nonconforming FEM for the pure displacement problem in linear elasticity is optimal and robust, SIAM J. Numer. Anal. 50 (2012) 1264–1283.
[7] R. Kouhia, R. Stenberg, A linear nonconforming finite element method for nearly incompressible elasticity and Stokes flow, Comput. Methods Appl. Mech. Engrg. 124 (1995) 195–212.
[8] D.N. Arnold, F. Brezzi, J. Douglas Jr., PEERS: a new mixed finite element for plane elasticity, Jpn. J. Appl. Math. 1 (1984) 347–367.
[9] D.N. Arnold, R. Winther, Mixed finite elements for elasticity, Numer. Math. 92 (2002) 401–419.
[10] M. Fortin, F. Brezzi, Mixed and Hybrid Finite Element Methods, Vol. 2, Springer-Verlag, New York, 1991.
[11] M. Lonsing, R. Verfürth, A posteriori error estimators for mixed finite element methods in linear elasticity, Numer. Math. 97 (2004) 757–778.
[12] C. Carstensen, F. Hellwig, Low-order discontinuous Petrov-Galerkin finite element methods for linear elasticity, SIAM J. Numer. Anal. 54 (2016) 3388–3410.
[13] P. Hansbo, M.G. Larson, Discontinuous Galerkin methods for incompressible and nearly incompressible elasticity by Nitsche's method, Comput. Methods Appl. Mech. Engrg. 191 (2002) 1895–1908.
[14] J. Huang, X. Huang, An *hp*-version error analysis of the discontinuous Galerkin method for linear elasticity, Appl. Numer. Math. 133 (2018) 83–99.
[15] E. Artioli, S. de Miranda, C. Lovadina, L. Patruno, A family of virtual element methods for plane elasticity problems based on the Hellinger-Reissner principle, Comput. Methods Appl. Mech. Engrg. 340 (2018) 978–999.
[16] L. Beirão da Veiga, F. Brezzi, L.D. Marini, Virtual elements for linear elasticity problems, SIAM J. Numer. Anal. 51 (2013) 794–812.
[17] A.L. Gain, C. Talischi, G.H. Paulino, On the virtual element method for three-dimensional linear elasticity problems on arbitrary polyhedral meshes, Comput. Methods Appl. Mech. Engrg. 282 (2014) 132–160.

[18] G. Harper, J. Liu, S. Tavener, B. Zheng, Lowest-order weak Galerkin finite element methods for linear elasticity on rectangular and brick meshes, J. Sci. Comput. 78 (2019) 1917–1941.

[19] C. Wang, J. Wang, R. Wang, R. Zhang, A locking-free weak Galerkin finite element method for elasticity problems in the primal formulation, J. Comput. Appl. Math. 307 (2016) 346–366.

[20] R. Wang, X. Wang, K. Zhang, Q. Zhou, Hybridized weak Galerkin finite element method for linear elasticity problem in mixed form, Front. Math. China 13 (2018) 1121–1140.

[21] R. Wang, Z. Wang, J. Liu, Penalty-free any-order weak Galerkin FEMs for linear elasticity on quadrilateral meshes, J. Sci. Comput. 95 (2023) 22, Paper (20).

[22] Y. Feng, Y. Liu, R. Wang, S. Zhang, A conforming discontinuous Galerkin finite element method on rectangular partitions, Electron. Res. Arch. 29 (2021) 2375–2389.

[23] Y. Wang, F. Gao, J. Cui, A conforming discontinuous Galerkin finite element method for linear elasticity interface problems, J. Sci. Comput. 92 (2022) 20, Paper (9).

[24] X. Ye, S. Zhang, A conforming discontinuous Galerkin finite element method, Int. J. Numer. Anal. Model. 17 (2020) 110–117.

[25] X. Ye, S. Zhang, A conforming discontinuous Galerkin finite element method: Part II, Int. J. Numer. Anal. Model. 17 (2020) 281–296.

[26] X. Ye, S. Zhang, A conforming discontinuous Galerkin finite element method: part III, Int. J. Numer. Anal. Model. 17 (2020) 794–805.

[27] J. Wang, X. Ye, A weak Galerkin finite element method for second-order elliptic problems, J. Comput. Appl. Math. 241 (2013) 103–115.

[28] I. Babuška, M. Suri, Locking effects in the finite element approximation of elasticity problems, Numer. Math. 62 (1992) 439–463.

[29] S.C. Brenner, L.R. Scott, The mathematical theory of finite element methods, in: Texts in Applied Mathematics, 3rd Ed., Vol. 15, Springer, New York, 2008.

[30] S. Chen, G. Ren, S. Mao, Second-order locking-free nonconforming elements for planar linear elasticity, J. Comput. Appl. Math. 233 (2010) 2534–2548.

[31] J. Hu, H. Man, J. Wang, S. Zhang, The simplest nonconforming mixed finite element method for linear elasticity in the symmetric formulation on n-rectangular grids, Comput. Math. Appl. 71 (2016) 1317–1336.

[32] L. Chen, J. Hu, X. Huang, Stabilized mixed finite element methods for linear elasticity on simplicial grids in $\mathbb{R}^n$, Comput. Methods Appl. Math. 17 (2017) 17–31.

[33] J. Hu, A new family of efficient conforming mixed finite elements on both rectangular and cuboid meshes for linear elasticity in the symmetric formulation, SIAM J. Numer. Anal. 53 (2015) 1438–1463.

[34] J. Hu, S. Zhang, A family of symmetric mixed finite elements for linear elasticity on tetrahedral grids, Sci. China Math. 58 (2015) 297–307.

[35] G. Fu, B. Cockburn, H. Stolarski, Analysis of an HDG method for linear elasticity, Internat. J. Numer. Methods Engrg. 102 (2015) 551–575.

[36] W. Qiu, J. Shen, K. Shi, An HDG method for linear elasticity with strong symmetric stresses, Math. Comp. 87 (2018) 69–93.

[37] B. Zhang, J. Zhao, Y. Yang, S. Chen, The nonconforming virtual element method for elasticity problems, J. Comput. Phys. 378 (2019) 394–410.

[38] Y. Liu, J. Wang, A locking-free P_0 finite element method for linear elasticity equations on polytopal partitions, IMA J. Numer. Anal. 42 (2022) 3464–3498.

[39] Y. Wang, F. Gao, The lowest-order weak Galerkin finite element method for linear elasticity problems on convex polygonal grids, Commun. Nonlinear Sci. Numer. Simul. 132 (2024) 12, Paper (107934).

[40] S.-Y. Yi, A lowest-order weak Galerkin method for linear elasticity, J. Comput. Appl. Math. 350 (2019) 286–298.

[41] J. Wang, X. Ye, A weak Galerkin mixed finite element method for second order elliptic problems, Math. Comp. 83 (2014) 2101–2126.

[42] J. Wang, X. Ye, A weak Galerkin finite element method for the Stokes equations, Adv. Comput. Math. 42 (2016) 155–174.

[43] X. Ye, S. Zhang, A conforming discontinuous Galerkin finite element method for the Stokes problem on polytopal meshes, Internat. J. Numer. Methods Fluids 93 (2021) 1913–1928.

[44] M. Dauge, Elliptic boundary value problems on corner domains, in: Smoothness and Asymptotics of Solutions, Vol. 1341, Springer, Berlin, 1988.

[45] P. Grisvard, Elliptic problems in nonsmooth domains, Soc. Ind. Appl. Math. (2011).

[46] L. Mu, X. Ye, S. Zhang, Development of pressure-robust discontinuous Galerkin finite element methods for the Stokes problem, J. Sci. Comput. 89 (2021) 25, Paper (26).

[47] H. Wei, Y. Huang, Fealpy: Finite Element Analysis Library in Python, Xiangtan University, 2017-2023, https://github.com/weihuayi/fealpy.

[48] F. Auricchio, L. Beirão da Veiga, C. Lovadina, A. Reali, An analysis of some mixed-enhanced finite element for plane linear elasticity, Comput. Methods Appl. Mech. Engrg. 194 (2005) 2947–2968.